

Yale University

EliScholar – A Digital Platform for Scholarly Publishing at Yale

Yale Medicine Thesis Digital Library

School of Medicine

1-1-2017

The Application Of Small Molecule Inhibitors Of Ngr1 And Lpa1 Towards The Goal Of Neuroregeneration In The Central Nervous System

Hiam Naiditch
Yale University

Follow this and additional works at: <https://elischolar.library.yale.edu/ymtdl>



Part of the [Medicine and Health Sciences Commons](#)

Recommended Citation

Naiditch, Hiam, "The Application Of Small Molecule Inhibitors Of Ngr1 And Lpa1 Towards The Goal Of Neuroregeneration In The Central Nervous System" (2017). *Yale Medicine Thesis Digital Library*. 2158.
<https://elischolar.library.yale.edu/ymtdl/2158>

This Open Access Thesis is brought to you for free and open access by the School of Medicine at EliScholar – A Digital Platform for Scholarly Publishing at Yale. It has been accepted for inclusion in Yale Medicine Thesis Digital Library by an authorized administrator of EliScholar – A Digital Platform for Scholarly Publishing at Yale. For more information, please contact elischolar@yale.edu.

The application of small molecule inhibitors of NgR1 and LPA1 towards the goal of neuroregeneration in the central nervous system

A Thesis Submitted to the Yale University School of Medicine in Partial Fulfillment of the Requirements for the Degree of Doctor of Medicine

by

Hiam Naiditch

2017

Abstract:

Disorders affecting the CNS are significantly disabling and often carry a poor prognosis of functional recovery. Pharmacotherapies that promote functional improvement via neuroregeneration have proven to be an elusive goal. Factors intrinsic to the neuronal microenvironment, particularly myelin-associated proteins such as Nogo-A, MAG, and OMgp, have been shown to be important in inhibiting such regeneration through neuronal NgR1. Additionally, LPA signaling through LPA₁ has also shown to be important in inhibiting neuroregeneration through mechanisms that are currently being researched.

It has been previously shown that application of a NgR1 decoy receptor (AA-NgR(310)ecto-Fc) increases sprouting below the site of the lesion in rats with spinal cord contusion injuries. Likewise, application of this same decoy receptor effectively disinhibited functional recovery as exemplified by the increase in percentage of weight-bearing rats treated with the decoy receptor. Noting the more ideal synthetic properties of a small molecule pharmaceutical, here we attempt to use a small molecule inhibitor of NgR1 to induce the *in vitro* regeneration of axons following scrape injury as well as in an *in vivo* model of mice with SCI. Additionally, noting the importance of LPA₁ as shown through previous studies, we also attempt to utilize a small molecule inhibitor of LPA₁ to promote axonal regeneration.

Our results show that inhibition of NgR1 with the small molecule inhibitor YU-NR-008 did not significantly improve axonal regeneration *in vitro*. Application of the NgR1 inhibitor YU-NR-008 alone showed a trend toward improved axonal regeneration, albeit insignificant (mean signal intensity for YU-NR-008 treated animals at 1.243 ± 0.128 vs. control 1.00 ± 0.00 , $p = 0.0787$). Co-treatment with YU-NR-008 and Nogo-22 did not rescue Nogo-22-mediated inhibition of axonal regeneration (Nogo-22 0.771 ± 0.051 vs. Nogo-22 with YU-NR-008 at 0.801 ± 0.073).

Additionally, functional recovery as measured by the Basso Mouse Scale (BMS) was not improved with the administration of YU-NR-008 following SCI for 2 or 4 weeks (D32 BMS scores were 4.643 ± 0.713 (SEM) for control vs. 3.550 ± 0.669 for animals treated with YU-NR-008 for 4 weeks). Likewise, administration of the LPA₁ antagonist AM095 did not improve functional recovery following SCI (mean BMS at 54 days for AM095-treated animals was 3.182 ± 0.532 vs. 5.033 ± 0.448 for vehicle-treated animals). We conclude that the tested doses of YU-NR-008 and AM095 were ineffective in promoting recovery in a rodent model spinal cord injury. Additional studies will be needed to determine whether axonal growth was stimulated by these doses, or if drug doses failed to achieve the cellular target effect following spinal cord injury.

Acknowledgements

Wisdom shouts jubilantly outside, it gives its voice in the streets (Proverbs 1:20).

Firstly, I would like to acknowledge and thank G-d, Whose presence in my life continue to lead to a fundamental appreciation of His work. I would also like to thank my family, particularly my wife, Chaya Sarah, whose encouragement and wisdom have helped me throughout my research year and beyond.

In addition, I would like to thank all the members of the Regeneration Group at the Strittmatter Lab: Xingxing Wang, MD; Yuichi Sekine, PhD; Maria Dell'Anno, PhD; Sarah Baghat, PhD; Will Cafferty, PhD; and Katie Fink, PhD for their teaching and for their assistance with methodology. I would also like to thank Tomoko Sekine-Konno, Charlene Bloch, Stefano Sodi, and Yiguang Fu for their tireless work in maintaining the functional integrity of the laboratory and for their assistance with animal studies. I would also like to thank all the members of the regeneration group for their teaching and for their friendship, particularly Levi Smith, PharmD.

For their guidance and for their assistance as members of my Thesis Committee, I would like to thank Hal Blumenfeld, MD, PhD and Peter Takizawa, PhD.

Finally, I would like to thank Dr. Stephen Strittmatter, whose belief in my abilities led me to embark on a research project I would not have otherwise conceived of as possible. His guidance kept me focused and dedicated throughout the year. I will always value my experience in his laboratory as one during which I was able to truly engage in the quest of scientific inquiry. I am grateful for his mentorship and guidance.

Table of Contents

Introduction.....	1
Statement of Purpose.....	12
Methods.....	13
Results.....	18
Discussion.....	23
References.....	32
Figure References and Legends.....	36

Introduction

Spinal cord injury (SCI) is estimated to affect about 250,000-300,000 people in the United States, with approximately 12,000 new cases each year, primarily in young adults aged 16-30 [1]. Causes can range from sports injuries to car accidents. Incomplete tetraplegia (indicating an injury at the cervical level) accounts for the most frequent neurologic status (40.6%) at discharge, with roughly 80% of patients still unemployed at one year post-injury [1].

In addition to the significant functional impact on the individual, there is a substantial financial cost to those with SCI and society at large. Depending on the level of injury, SCI can cost as much as \$350,000-\$1,000,000 per patient in the first year alone, with a lifetime cost of \$1 million-\$4.5 million for patients, which does not include lost wages due to unemployment [1]. Patients who suffer from SCI thus encounter a drastic paradigm shift in level of function and financial stability at a time in their lives typically associated with opportunity and potential. Research that could improve the functional outcome of such patients is therefore much needed.

The facilitation of functional recovery for those with SCI, however, has proven to be an elusive goal. For one, post-developmental neuroplasticity is rare in the CNS, as noted as early as 1927 by Ramon y Cajal [2, 3]. The functional reason behind such stability has been hypothesized to be due to the need for preservation of existing neural networks for efficient higher order functions [3]. Numerous mechanisms for how this might occur have been extensively studied and include factors intrinsic to neurons such as GAP-43, cAMP, PTEN, mTOR, KLF4, and SOCS3 [4]. Past research has emphasized, however, that it is not only the CNS neurons themselves that prohibit the type of regeneration typically seen in the PNS, but also the environment in which the neurons find themselves in [4, 5]. In a series of seminal studies, Aguayo et al. showed that CNS neurons can regenerate their axons through peripheral nerve grafts and become

ensheathed in Schwann cells [5]. Similarly, PNS neurons do not have the same regenerative capacity in a CNS glial environment, highlighting the importance of the microenvironment even in the presence of factors intrinsic to the neuron [5].

A number of mechanisms have been proposed to explain the environmental dependence of neuroregeneration. Glial scar tissue that form in the CNS can physically block the normal regrowth of axons into the site of injury, with chondroitin sulfate proteoglycans (CSPGs) playing an important molecular role in the inhibitory process [6, 7]. Premature synapse formation may prevent restoration of functional neural circuitry [8]. Following the experiments of Aguayo et al, Savio et al showed that homogenates of CNS myelin could block growth cones and neurite extension *in vivo*, implicating oligodendrocytes and the unique CNS myelin sheath they form as important inhibitors of neuroregeneration [9]. Subsequent studies led to the discovery of many of the molecular signaling elements responsible for myelin-mediated inhibition of CNS regeneration, and include Nogo-A, Oligodendrocyte Myelin Glycoprotein (OMgp), myelin-associated glycoprotein (MAG), ephrin-B3, and Semaphorin 4D [10]. This molecular milieu is largely unique to CNS myelin [10]. Importantly, three of these myelin-associated inhibitors (Nogo-A, OMgp, and MAG) have been shown to interact with the neuronal Nogo-66 Receptor 1 (NgR1) as well as paired-immunoglobulin like receptor B (PirB), both of which have been implicated in inhibition of axonal outgrowth [10, 11].

NgR1 is the best-studied member of a family of three related (NgR1, 2 and 3) GPI-anchored receptors located on neurons which have been shown to participate in inhibition of axon growth [12]. NgR1 can be found on neuronal axons as well as pre- and post-synaptic locations, and is typically found co-localized with Nogo-A [13]. NgR1 knockout mice show enhancement of rubrospinal and raphespinal neuronal tract regrowth after injury [14]. When NgR1 is bound to ligand (which may include CSPGs), a complex is formed with the co-

receptors/signal transducers LINGO-1 and p75^{NTR} or TAJ/TROY, which—possibly via protein kinase C—ultimately activates the RhoA/ROCK pathway, as shown in Figure 1 [3, 12, 15-17]. Activation of the RhoA/ROCK pathway leads to actin regulation and concomitant growth cone collapse and inhibition of neurite outgrowth, thus prohibiting neuroregeneration of damaged neuronal processes or sprouting of fibers from intact axons [18]. Specifically, activation of the GTPase RhoA via binding with GTP leads to downstream activation of the Rho-associated kinases (ROCK) I and II (ROCK II being primarily expressed in the brain and muscle tissue) [19].

Current understanding implicates F-actin as playing a prominent role in the extension of filopodiae and lamellipodiae that characterize growth cones [20, 21]. In the growing axon, F-actin undergoes polymerization at the distal growth cone while its proximal end is simultaneously retracted by myosin II towards the center of the axon, exhibiting an elegantly balanced process whose fate depends largely on external cues [21, 22]. Although the exact mechanism through which the RhoA/ROCK pathway mediates growth cone collapse remains a subject of study, growth cone collapse tends to halt axon extension and may lead to axonal retraction [20]. ROCK has been shown to be implicated in shutting down F-actin polymerization at the distal growth cone, and may also mediate axonal retraction by promoting the formation of F-bundles of F-actin, with retraction of the axon mediated by the action of myosin II through such newly formed bundles [21]. ROCK has been shown to be directly implicated in activation of myosin II via phosphorylation of regulatory myosin light chain regions [21]. In addition, ROCK prevents the dephosphorylation of the myosin light chain (and thus facilitates continued activation) via phosphorylation of the myosin binding subunit that anchors protein phosphatase 1 (also known as myosin light chain phosphatase, MLCP) to myosin [22]. Thus, inhibiting NgR1-mediated RhoA/ROCK activation represents a promising target to allow for facilitation of axonal

regrowth. Importantly, NgR1 has also been implicated in stabilizing the anatomy of the developing brain and limiting plasticity, likely through similar mechanisms [23].

Among the known ligands for NgR1, Nogo-A appears to have the most well-studied, functionally significant role in NgR1-mediated neuronal outgrowth inhibition. Following SCI, Nogo-A knockout mice showed improved (but strain-dependent) raphespinal and corticospinal tract regrowth, whereas OMgp and MAG knockout mice did not [10, 24-26]. Interestingly, triple knockout of Nogo-A, MAG, and OMgp did not promote functional recovery as measured by grid walk test when compared to wild type mice following lateral hemisection [26].

Nogo-A, also known as Reticulon-4A is the largest member of the Nogo family, and the only isoform naturally found in myelin [10, 27]. It is a 200kD protein composed of a C terminal, two transmembrane domains, and an extracellular N terminal [27]. Following CNS injury, Nogo-A expression follows a predictable temporal expression pattern: At first, expression is downregulated as compared to baseline. Then, at 7 days post-injury, Nogo-A expression shoots up to roughly twice that of baseline levels [28]. While full-length Nogo-A is typically found in CNS tissue before and after damage, certain segments have been implicated in mediating its inhibitory effects: A 66 amino acid loop (Nogo-66) as well as the amino terminus itself have both been implicated in inhibition of axonal regeneration, although the amino terminus works through disruption of integrin function rather than via NgR1 [10, 28-30].

Various methods have been attempted to restore function following CNS injury, including neural bypass, stem cell implantation, each undergoing active research with varying degrees of success [2, 31, 32]. Given the importance of NgR1-mediated inhibition via Nogo-A and other MAIs, however, it is conceivable that functional recovery can be mediated by pharmacologically facilitating regeneration of the injured axons, or, perhaps, forming new

collaterals from uninjured neurons [33, 34]. Indeed, this pathway has been extensively targeted in our own laboratory and in others [18, 33-35]. Inhibition of downstream RhoA/ROCK can help disinhibit myelin-mediated inhibition, but may have unintended inhibitory effects on neuronal motility [33]. Antibodies that target Nogo and a peptide NgR antagonist, while effective, only inhibit the interaction of Nogo and not OMgp or MAG and have unknown anti-myelin effects [15]. Perhaps the most potent inhibition of the NgR1 pathway has been demonstrated via intrathecal administration of the Nogo decoy receptor NgR(310)ecto-Fc following dorsal hemisection of the spinal cord, which was shown to enhance the growth of CST fibers in a functionally significant manner Figure 2 [33]. Rats so treated showed functional recovery as measured by improved locomotion that correlated with histological evidence of sprouting of axons of the corticospinal and raphespinal tracts, findings that led to testing of the agent in primates [15]. It is with the understanding of the significance of this pathway that a small molecule inhibitor of the interaction of MAIs and NgR1—with its ease of synthesis, potential for manipulation of solubility, potential for biologic stability, and lower cost of production—was sought.

A number of methods were employed by our laboratory to find a small molecule inhibitor of the MAI/NgR1 interaction. High throughput screening with functional assays measured neurite outgrowth and revealed a number of promising molecules, but it was *in silico* screening—whereby the docking on the NgR1 of roughly 2,000,000 small molecules is tested based on biochemical and physical properties—that yielded a molecule known as YU-NR-008 that showed perhaps the most promise. A DELFIA assay testing the ability of YU-NR-008 to inhibit the binding of NoGo-66 to NgR1 (as represented by the analog decoy receptor NgR(310)ecto-Fc noted above) revealed that the compound shows dose-dependent inhibition, with the IC₅₀ in a reasonable range (roughly 1 μ M). Further studies performed by Levi Smith, PhD

showed that the compound could be administered intraperitoneally and reach steady-state levels that were pharmacologically significant (unpublished).

Neuroplasticity is broadly defined as “changes in neuronal structure and function, including synaptic changes as well as modifications in neural pathways” [36]. It follows, then, that neuronal plasticity is not just confined to circumstances where neuronal processes are injured and must regenerate, but also to instances where more subtle neuronal changes may be evident, such as in normal anatomic development as well as in learning [23, 37]. Indeed, similar mechanisms involving NgR1-mediated signaling are responsible for the subtle changes found in development as in robust neuroregeneration [23]. Neuroanatomical plasticity in development (as measured by turnover of dendritic spines and axonal varicosities) is normally stabilized in mice at age 45 days, but *ngr*^{-/-} mice maintain an adolescent-like plasticity through 180 days [23]. Conditional deletion of *floxed ngr1* also restores dendritic spine turnover to adolescent levels [23].

Perhaps in a more nuanced manner, NgR1 signaling has also been implicated in experimental learning paradigms [37]. The location of NgR1 at synapses—aside from axons, where their presence suggests a role in axonal regrowth—suggests an additional role in synaptic plasticity, which is also important in learning [13, 38, 39]. Recent experiments showed that antibody-mediated blocking of Nogo-A/NgR1 signaling increased long term potentiation (LTP) induced by stimulation of horizontal cortical fibers [40]. Intrathecal administration of a Nogo-A blocking antibody led to increased dendritic spine density as well as more effective learning of a novel pellet-grasping task [40]. Thus, NgR1 signaling has been implicated in a spectrum of behavioral paradigms requiring varying degrees of neuroplasticity. One such paradigm, fear conditioning and extinction, represents a rapid, functionally important method of testing pharmacologically-mediated interruption of Nogo-A/NgR1 signaling.

Fear conditioning is a classic experimental model whereby a neutral stimulus (e.g. a tone) is paired with an aversive stimulus (e.g. electrical shock) with the eventual outcome that the neutral stimulus is experienced as aversive [41]. Fear conditioning thus follows a classical/Pavlovian conditioning paradigm, the neuroanatomical basis of which has been well-studied [41]. Following fear conditioning, the conditioned stimulus can be provided without the aversive, unconditioned stimulus, leading to a decreased fear response [42]. This process is called *fear extinction*, whereby memory erasure of a learned association can effectively occur [43]. Learned fears are much more readily extinguished in rodents still in their developmental stage, but fears in adults tend to be much more difficult to “erase” (likely due to CSPGs organized into structural CNS elements known as *perineuronal nets*) [43]. Experiments by Akbik et al have shown that *ngr*^{-/-} mice display a phenotype more similar to juvenile mice as compared to wild type [23]. *Ngr*^{-/-} mice experience more rapid extinction than wild type (although, interestingly, no significant difference was noted in initial conditioning) [23]. Following fear extinction, previously learned fears can be recovered through retraining, typically at a rate faster than in mice who have not undergone an initial conditioning/extinction protocol [37]. Recently, Bhagat et al also showed that *ngr*^{-/-} mice recover previously learned fears at a rate similar to wild type mice who had never been conditioned [37]. Results were similar for conditional *flox*-mediated deletion of *ngr* [37].

The experimental design for fear extinction and retrieval requires 10 days in total, which is ideal for a study that could test the pharmacologic inhibition of a small molecule inhibitor of NgR1 signaling in an effort to promote neuroplasticity. Indeed, preliminary studies using YU-NR-008 showed that while mice treated with 30mg/kg/12hr starting from the second day showed a similar rate of extinction vs. control (with YU-NR-008-treated animals showing an insignificant trend towards a more rapid rate of recovery), mice treated with the drug showed a significant

decrease in fear recovery vs. control as measured by percentage of mice showing the fear response (unpublished; Figure 3). Given these promising results, a series of experiments were devised that would employ YN-NR-008 towards the purpose of disinhibiting axonal regeneration in both an *in vitro* neuronal injury model and *in vivo* model of SCI. These experiments are described in this thesis.

AM095

Efforts to promote neuroregeneration of damaged neurons have been complimented by attempts at minimizing the damage to the CNS that occurs following injury, also called neuroprotection [44]. Injury to tissue can occur via direct mechanical damage as well as via the cascade of physiologic responses that occur following the primary injury [44]. Inflammation in the CNS may also be prolonged, further exacerbating the initial damage to the spinal cord [45]. Interestingly, a more robust inflammatory response occurs in the spinal cord than in the brain [46]. Glial scarring, as mentioned above, can impede functional recovery in mammalian species [6, 7, 47]. The CNS is shielded from typical systemic immune responses by the blood-brain barrier, and the inflammatory cascade in the CNS is uniquely different from other organ systems, in spite of production of cytokines similar to those organ systems (e.g. IL-1 β and TNF α) [45, 48, 49]. Microglia are native to the CNS immune cell milieu but other cells like macrophages and (less often) neutrophils may be recruited to the area [50].

Given the prohibitive role of secondary injury in functional recovery, approaches that seek to target the inflammatory response and protect the CNS from an overly ambitious immune response have been attempted, with limited success [50]. Corticosteroids like methylprednisolone show only modest benefit, and carry the risk of secondary complications [50]. Ibuprofen has been shown to promote corticospinal and raphespinal sprouting after spinal

cord injury [10]. However, this effect has been shown to be mediated through RhoA/ROCK signaling rather than strictly through the drug's anti-inflammatory properties [10]. In fact, there are elements of the immune response that are important for functional recovery [50]. When neutrophils—thought to be toxic to CNS tissue due to their release of elastase and reactive oxygen species—are depleted by Ly6G/Gr-1 antibodies, less white matter is spared and worse functional outcomes ensue [51]. It is thought that these negative effects may be mediated through a decrease in factors important for normal wound healing, including bone morphogenic proteins (BMP), vascular endothelial growth factors (VEGF), and neurotrophic factors (NTF) as well as slowed astrocytic reactivity (which is normally associated with a wound healing response) [51]. In addition, certain subsets of immature myeloid immune cells—called myeloid-derived suppressor cells (MDSC), which are also Gr-1⁺—may play a suppressive role in inhibiting T cell responses [50]. Notably, the depletion of Gr-1⁺ monocytes leads to less robust functional recovery in mice with SCI, and Gr-1⁺ monocytes recruited from outside of the blood-brain barrier appear to be necessary for normal functional recovery following SCI [52]. Intriguingly, macrophages of the M2 phenotype have been shown to increased neurite outgrowth as opposed to their M1 counterparts [50]. It is evident, then, that the immune response is a sophisticated network of events, some with positive effects towards functional healing, and others that do not benefit functional recovery. A nuanced approach is thus required in targeting the immune response towards the goal of functional recovery.

Within the network of immune interactions taking place following SCI, the targeting of one pathway has shown increasing promise. Lysophosphatidic acid (LPA) is a ubiquitous bioactive lipid that takes part in cell proliferation and migration, cytokine and chemokine release, and prevention of apoptosis [53, 54]. LPA mediates its effects through at least six 7-transmembrane, heterotrimeric G protein-coupled receptors, LPA₁₋₆ [53]. Cells of the CNS

microenvironment express different receptors, with neurons generally expressing LPA₁ and—more abundantly—LPA₂; astrocytes expressing LPA₁ and LPA₅, with upregulation of LPA₁ and LPA₂ following SCI; LPA₁ and LPA₃ expressed in microglia, the latter of which is upregulated in a model of neuroinflammation; and on oligodendrocytes, both LPA₁ and LPA₃ are expressed [55]. LPA levels have been shown to increase following SCI, and exogenous LPA exposure has been shown to cause demyelination, likely through interactions with LPA₁ on microglia [54]. Thus, LPA-mediated signaling represents an intriguing target with the goal of mediating secondary damage due to neuroinflammation.

Recently, Santos-Nogueira et al showed that, in addition to being upregulated following SCI, the inhibition of LPA₁ with a selective antagonist known as AM095 prevents the demyelination otherwise seen with exogenous administration of LPA [54]. AM095 is a potent LPA₁-selective antagonist (with IC₅₀ values less than 1μM) that has high oral bioavailability, a half-life of 1.5 hours, and has been shown to be well-tolerated in rats and dogs [56]. Prior experiments performed by Swaney et al in 2011 showed that AM095 decreased pathologic bleomycin-induced pulmonary fibrosis as well as renal fibrosis following ureteral obstruction in multiple animal models, but did not affect normal wound healing [56]. Recently, Santos-Nogueira et al also showed that AM095 (administered orally 1hr post-SCI and subsequently every 12 hours at 30mg/kg for one week) promotes functional recovery of mice following SCI, as measured by a standardized motor test, the Basso Mouse Scale (BMS) [44]. Interestingly, AM095 did not affect microglia counts or infiltration of macrophages [44]. An inhibition of demyelination was seen with the treatment, but little neuronal sparing was noted [44].

Interestingly, the LPA/LPA receptor pathway is also implicated in neurite retraction—LPA₄, for one, can exert its effects through the Rho/ROCK pathway, as can LPA₁ [53, 54, 57]. LPA is also present in the developing brain, with receptor expression following a predictable time

course [55]. In addition, the expression of *lpar1*, the gene responsible for LPA₁ expression, was found to be significantly downregulated in sprouting neurons following a corticospinal tract lesion (pyramidotomy) (Fink et al, submitted abstract). The importance of the role of LPA₁ in axonal regeneration was further highlighted when animals received the LPA₁ antagonist AM095 following a pyramidotomy lesion and were found to exhibit significantly enhanced sprouting of neurons into the contralateral ventral horn (Fink et al, submitted abstract). Furthermore, those animals that were treated with AM095 exhibited a greater degree of functional recovery than controls as measured by a grid-walking test (Fink et al, submitted abstract). It is thus intriguing to consider that interfering with LPA signaling may also lead to more robust axonal regeneration following SCI. For our experiments, we sought to initiate AM095 administration at a later time and treat mice with SCI for a longer period of time in an effort to isolate neuro-regenerative effects of LPA₁ blockade. The following thesis presents the results of this experiment.

Statement of Purpose

Our goal was to employ small molecule antagonists of receptors known to be important in inhibiting sprouting of intact and injured axons for the purpose of regeneration of injured axons.

Specifically, we hypothesized that application of a small molecule (YU-NR-008, a.k.a. "Go") enhances/disinhibits axonal regeneration via an NgR1-mediated mechanism in a functionally significant manner. Our intent was to utilize a small molecule inhibitor for the pharmacologic inhibition of NgR1 towards these specific aims:

1. Observe *in vitro* disinhibition of axonal regeneration upon application of Go in the presence of an endogenous inhibitor (NoGo-22).
2. Observe improved recovery of function as well as rate of functional recovery in an *in vivo* model of SCI.

Additionally, we hypothesized that administration of the LPA₁ inhibitor AM095 would lead to improved functional recovery and rate of recovery following SCI when administered at 30mg/kg/12hr, beginning 24 hours for a total of 20 days. This time course was chosen in an attempt to isolate neuroregenerative effects from neuroprotection from damage primarily secondary to inflammation. Specifically, we sought to observe improved recovery of function as well as rate of functional recovery in an *in vivo* model of SCI upon application of AM095.

Methods

***In Vitro* CNS Injury Model/Scrape Assay**

Cell Culture

For our primary *in vitro* neuroregeneration assay, C57Bl/6 pregnant female mice with E17-E18 embryos were sacrificed. Brains of the embryonic mice were dissected and cortical neurons from both hemispheres were isolated and placed into Hibernate E –CaCl₂ medium (BrainBits). Following aspiration of medium, cortical neurons were placed into an enzyme solution containing Mg/Ca-free HBSS (4mL), papain (96μl), EDTA (25μl), CaCl (7.5μl), and DNase (10mg/mL, 500μl) for 20-30min. of incubation. Subsequently, tissue was washed once with 10ml HBSS and twice with 10ml Neurobasal-A medium with additives (500ml Neurobasal medium (NB-A), 5ml of 1% Pen-strep, 5ml Na-Pyruvate (1mM), 5ml GlutaMax (2mM), and 10ml B-27 supplement). The tissue was then homogenized by repeated pipetting and was subsequently filtered through a 40μm cell strainer. This cell solution was then diluted 38:1 in Neurobasal-A solution (noting that one pup brain provides confluent coverage of neurons for 3 plates) and was subsequently placed into the 60 central wells of a 96-well plate at a volume of 200μl/well, with the outermost wells containing sterile water. Each plate was divided into four quadrants to represent each condition, and each experiment was repeated 4 times (on 4 different plates), allowing for rotating of the quadrants to allow for greater power and to avoid potential bias introduced via location in incubator. The cells were allowed to grow in culture for 7-16 days, depending on the experiment, with medium changed at 7 days. Scrape injury was performed at 7-16 days using a 96-well special scraping tool made for this purpose (V&P Scientific) and 150μl of medium was removed from each well. Subsequently, 50μl of relevant condition was placed: Control containing a solution of 8% DMSO, 46% PEG 400, and 46% of 10% cyclodextrin in H₂O at

a concentration of 100nM-1 μ M in Neurobasal-A medium; Nogo-22 (10nM-300nM); 1mg Go dissolved in the same solution used for control at concentrations of 100nM-10 μ M; and Go with Nogo-22 at indicated concentrations).

Nogo-22 is a 22kDa isolated fragment of Nogo-A that contains three important inhibitory components: Nogo-66, Nogo-A-24, and Nogo-C39 [58]. It has been shown to be a more potent suppressor of axon regeneration than Nogo-66 alone in previous experiments performed by Huebner et al [58]. We thus sought to use Nogo-22 in an effort to test competitive inhibition with our small molecule inhibitor YU-NR-008.

Neurons were allowed to sit for 3-7 days with relevant condition, and were subsequently fixed using 4% PFA in PBS, made permeable with 0.1% Triton, and then stained using anti- β III microtubulin overnight. Subsequently, Alexa Flour-488 donkey anti-mouse antibody (Life Technologies) was applied along with DAPI (Cell Signaling Technologies) and rhodamine phalloidin (Life Technologies) for imaging.

Imaging

Images were obtained via fluorescent microscopy using ImageExpress Micro XL. Images were then cropped using ImageJ (NIH) to capture only the area of axonal regeneration. Subsequently, individual images were run through a MatLab (R2012b) program that records Alexa-Flour 488 (green) signal above a preset threshold intensity. Typically, each experimental condition was repeated on four plates, with quadrants rotated to account for any discrepancy in location on the plate and in the incubator. Means for each quadrant were normalized to the mean of the vehicle treated neurons given substantial variation from plate to plate based on previous experience in the laboratory, making it difficult to compare from one plate to another. Means were calculated and compiled using Excel (Microsoft), and the means were then used as data

points in the final analysis for statistical significance via 2-way ANOVA using statistics computing software (GraphPad Prism 6).

***In vivo* mouse SCI model**

Surgery

11-12 week old female C57Bl/6 animals were placed under anesthesia using 1-5% isoflurane. Location for the incision and subsequent T7-T9 laminectomy was determined by using the *vertebra prominens* as an anatomical landmark in mice for T10. Following the incision, paraspinous muscles were dissected using small scissors to reveal the spinous process of T7-T9 and associated lamina. Microscissors were used to perform a bilateral laminectomy to reveal the spinal cord. Curved iridectomy scissors were then used to perform a dorsal hemisection to a depth of 1.1mm. The incision site was subsequently closed using an intramuscular suture followed by 3-4 skin sutures (4-0 Vicryl; Ethicon). Pain relief was provided using buprenorphine. Penicillin was used for antibiotic prophylaxis.

Post-operative animal care was performed through twice daily bladder expression for the first 7-14 days, followed by once daily thereafter. Routine post-operative care was performed and animals were regularly weighed following the procedures.

Treatment Protocols

Go injections (3-6mg/mL as a suspension in sunflower oil) and control (sunflower oil alone) injections began at 3 days post operatively at a dose of 30mg/kg/12hr and continued for 2-4 weeks.

AM095 was suspended in normal (0.9%) saline with 1% DMSO to a final concentration of 3mg/mL. To ensure adequate dissolution, the mixture was sonicated for 10 minute intervals 3 times at 37°C. Treatment began 24 hours after dorsal hemisection for 20 days.

Assessment of functional recovery

To assess for functional recovery, hind leg movements were assessed according to the Basso Mouse Scale (BMS) [59]. Animals were observed for BMS first on D3 post-spinal cord injury (SCI), and thereafter once weekly. Animals were randomized to control and treatment groups based on the initial D3 BMS measurement.

For AM095-treated animals, BMS measurement were performed roughly 24 hours post-operatively, on D3, and subsequently every 7-8 days. Control and treatment groups were randomized according to baseline BMS on D1.

Corticospinal tract tracer injection

On D38 of all experiments, animals were brought to the surgery room and anesthetized with 1-5% isoflurane as above. Anesthetized animals were affixed to a stereotaxis apparatus, and, following scalp incision, 5 burr holes were drilled using a micro-drill (Foredom) on the R lateral side of bregma (burr hole 1 at 2mm lateral, 1mm anterior to the frontal suture; burr hole 2 at 1mm lateral, 0.5-1mm posterior to the frontal suture; burr hole 3 at 3mm lateral, 1mm posterior to the frontal suture; burr hole 4 at 1mm directly posterior to burr hole 2; burr hole 5 at 1mm directly posterior to burr hole 3. A 30G needle was used to puncture the skull at the areas of the burr holes, taking care not to puncture the dura. A stabilized microsyringe with a pump controller (World Precision Instruments) was used to inject 75nl 10% BDA 0.7mm deep to the dura at a rate of 75nl/min at each burr hole site.

Alternatively, a craniectomy was performed using a micro-drill (Foredom) starting 1mm lateral to bregma and posterior to the frontal suture and extending 2mm anteriorly; then laterally to 3mm lateral to bregma, 1mm anterior to the frontal suture; from that point, drilling was extended 2mm directly posteriorly; drilling was then continued in the medial direction for 2mm to reach the original drilling site. Forceps were used to remove the incised skull and to expose the dura mater. 5 BDA injections were administered in a similar orientation to the burr hole protocol. Animals were subsequently sutured and were placed on a heating pad for recovery following cessation of anesthesia. Ampicillin and buprenorphine in LR were administered per protocol.

Histologic Analysis

On D56 animals were euthanized and subsequently perfused via intracardiac perfusion with chilled normal saline for 3-5 minutes for exsanguination and subsequently with chilled 4% PFA in PBS for 3-5 minutes. Spinal cords were then obtained and stored in 4% PFA in PBS for future analysis and imaging.

Experimenters

The initial dorsal hemisections for the 2 week-Go treated SCI experiments were primarily performed by Xingxing Wang, MD. The first surgery and harvesting of E18 mouse cortical neurons was performed by Yuichi Sekine, MD. Aside from these, the following experiments and data analysis were primarily performed by Hiam Naiditch under the guidance of Yuichi Sekine, PhD (cell culture/Scrape Assay) and Xingxing Wang, MD (animal surgeries and tissue preparation for forthcoming histological analysis). Basso Mouse Scale measurements require more than one observer. Special thanks to Tomoko Sekine-Komo, Maria Dell'Anno, PhD, Yuichi Sekine, PhD and Xingxing Wang, MD for assisting with these measurements.

Results

Nogo-22 inhibits axonal regeneration

Nogo-22 is a 22kDa fragment of Nogo-A that contains the three inhibitory regions Nogo-66, Nogo-A-24, and Nogo-C39. Nogo-22 has been previously shown to inhibit the outgrowth of neurons more potently than Nogo-66 alone [58]. Our experiments confirmed that Nogo-22 significantly inhibits the outgrowth of neurites when applied to neurons at 7 DIV for 3, 5, and 7 days of treatment. Figure 4a is a representative image showing Nogo-22 mediated inhibition on axonal regeneration into the scrape area vs. control. As shown in Figure 4b, Nogo-22 potently inhibits axonal regeneration when applied for three (mean fluorescent antibody signal intensity 0.788 ± 0.043 for Nogo-22-treated (n=16) and 1.00 ± 0.00 (n=20) for vehicle-treated (data are normalized), five (0.683 ± 0.123 for Nogo-22 (n=16) and 1.00 ± 0.00 for vehicle; n=16) and seven days (0.416 ± 0.049 for Nogo-22 (n=8) and 1.00 ± 0.00 for vehicle treated; n=8). Data represent relative intensity of signal normalized to vehicle from a fluorescent antibody to β -III tubulin (found in axons) and are displayed as means with standard errors of the mean and were analyzed by 2-Way ANOVA using GraphPad Prism 6 statistical software.

Importantly, neurons kept in culture with Nogo-22 for longer led to a greater degree of inhibition, as shown in Figure 4b. The importance of time of application of Nogo-22 has been previously shown in a similar experiment performed by Huebner et al, and suggests the role of Nogo-A/NgR1 signaling in development of stable neural networks in the CNS [58]. Our experiments suggest additionally that the amount of time of application of Nogo-22 may allow for greater Nogo-22-mediated inhibition, presumably also via the upregulation of NgR1.

YU-NR-008/Go is non-toxic to neurons

As shown in Figure 5a, following culture of neurons for 7DIV, application of 100nM of the NgR1 inhibitor Go for treatment for 3, 5 and 7 days shows a trend towards improvement in axonal regeneration as compared to control, although this trend is not significant. Similarly, increasing the concentration of Go to 1 μ M and applying to cultures at 7DIV for 3 days for varying days in treatment did not yield significant improvement in axonal regeneration. As shown in Figure 5b, at 3 days of treatment with 100nM Go, Go-treated neurons showed a relative β -III tubulin signal of 1.296 ± 0.150 (n=16) vs. vehicle treated (1.000 ± 0.000 ; n=12). At 5 days, Go-treated neurons were 1.290 ± 0.140 (n=12) vs. vehicle treated (1.000 ± 0.000 ; n=8). At 7 days, Go-treated neurons were 1.357 ± 0.271 (n=4) vs. 1.000 ± 0.000 for vehicle-treated (n=4).

Considering the potential role of YU-NR-008/Go as a competitive antagonist, we sought to increase the concentration of Go to override Nogo-22 mediated inhibition. We also sought to determine the effects of this concentration on neurons treated only with Go as compared to control. As shown in Figure 5b, application of 1 μ Go for 3 days of treatment beginning at 7DIV yielded a mean signal intensity of 1.140 ± 0.184 (n=8) vs. vehicle (1.000 ± 0.000 ; n=8). At 5 days, Go-treated showed a mean signal intensity of 1.417 ± 0.167 (n=12) vs. control (1.000 ± 0.000 ; n=8). At 7 days, Go-treated were 1.054 ± 0.253 (n=4) vs. vehicle (1.000 ± 0.000 ; n=4). Thus, increasing the concentration of Go does not appear to increase axonal regeneration in the absence of exogenous Nogo-22.

Noting that expression of NgR1 increases with the age of the neurons (Figure 6c, courtesy of Yuichi Sekine, PhD), we sought to optimize the experiment by increasing days in vitro prior to application of Go. Similar to the above results, following culture of neurons for 13DIV, application of 1 μ M Go for a 3-day treatment promotes a trend towards improvement in axonal regeneration as compared to control (fold change of 1.243 ± 0.128 (SEM) for Go-treated vs. 1.00 ± 0.00 for vehicle), although this trend is not significant (p=0.0787) (Figure 6a). Likewise,

treatment of neurons cultured for 16DIV did not yield improvement in axonal regeneration as compared to control. Figure 5c is a representative image showing the increase in axonal regeneration with Go application.

Treatment with the NgR1 inhibitor YU-NR-008/Go does not rescue Nogo-22-mediated inhibition of axonal regeneration

We sought to model the interaction of endogenous MAIs with NgR1 in the presence of the small molecule NgR1 inhibitor YU-NR-008/Go. To test whether Go inhibited binding of Nogo-22, we employed varying concentrations of the drug and the surrogate ligand for varying number of days.

As shown in Figure 6a, co-administration of 100nM Nogo-22 and 100nM Go at 7DIV did not lead to reversal of Nogo-22-mediated inhibition of axonal regeneration. For instance, at 7 days of treatment, neurons co-treated with Go and Nogo-22 (0.484 ± 0.066 ; n=4) and Nogo-22 alone (0.480 ± 0.082) experienced a similar inhibition of axonal regeneration.

Likewise, increasing the number of days in an attempt to account for increasing NgR1 expression as development progresses did not lead to a reversal of Nogo-22 mediated inhibition of axonal recovery. As shown in Figure 6b, o-administration of 300nM Nogo-22 and 1 μ M Go at 13DIV did not lead to reversal of Nogo-22-mediated inhibition of axonal regeneration. As expected, treatment with Nogo-22 yields significant inhibition (Nogo-22 0.771 ± 0.051 (SEM) vs. control 1.00 ± 0.00 , p=0.00434). Co-treatment with Go and Nogo-22 did not lead to rescue of Nogo-22-mediated inhibition of axonal regeneration (Nogo-22 0.771 ± 0.051 vs. Nogo-22 with Go 0.801 ± 0.073).

In an attempt to assess whether Go worked as a competitive inhibitor in the presence of Nogo-22, we also sought to use varying ratios of Nogo-22 to Go (See Figure 6d). Previous experiments have shown that a concentration of 310nM is sufficient in inducing a noticeable difference in axon regeneration, but as little as 1nM may induce growth cone collapse [58]. As shown in Figure 6c, the application of Go in the presence of 200nM Nogo-22 did not allow for rescue of Nogo-22-mediated inhibition of neuroregeneration (0.771 ± 0.051 for Nogo-22 vs. 0.801 ± 0.073 , $p=0.746$). Figure 6e shows a representative image showing the difference in regeneration following treatment with 100nM Go vs. control. Thus, treatment with YU-NR-008/Go alone does not appear to antagonize Nogo-22-mediated inhibition of axonal regeneration.

2-week and 4-week treatment with Go does not appear to improve functional recovery following SCI

For the in vivo studies, as shown in Figure 7d, 2-week treatment with Go at 30mg/kg/12hr did not appear to promote functional recovery following dorsal hemisection as measured by the Basso Mouse Scale (BMS). For instance, at D39 mean BMS for Go-treated animals was 2.40 ± 0.46 (n=10) vs. 1.667 ± 0.479 for control (n=9).

To determine whether increases the time of exposure to drug following SCI would promote neuroregeneration, the experiment was repeated, this time with treatment for 4 weeks. As shown in Figure 7e, 4-week treatment with Go at 30mg/kg/12hr did not appear to promote functional CNS recovery following dorsal hemisection as measured by the BMS. For example, the differences between D32 BMS scores (4.643 ± 0.713 (SEM) for control vs. 3.550 ± 0.669 for Go-treated animals) or D39 (4.071 ± 0.561 (control) vs. 3.35 ± 0.624) were not significant. Data represent means with SEM; statistical analysis was performed using GraphPad Prism and

employed 2-way ANOVA. Figures 7a, b, and c provide cross-sectional and sagittal views portraying the nature of the dorsal hemisection lesion [60, 61].

Administration of the LPA₁ antagonist AM095 does not appear to contribute to functional recovery via axonal sprouting

We sought to test the hypothesis of whether the application of the LPA₁ antagonist AM095 would rescue LPA-mediated inhibition if AM095 were applied after the inflammatory cascade had begun in an attempt to isolate the neuroregenerative effects of AM095. As seen in Figure 8a, initiating treatment with AM095 at 24 hours post-SCI for 20 days did not appear to improve functional recovery as compared to control. For example, mean BMS at 54 days for AM095-treated animals was 3.182 ± 0.532 (n=11) vs. 5.033 ± 0.448 for vehicle-treated animals (n=15).

Given the potential for skewed data with a disproportionate number of abnormally high baseline performers (as in D3 baseline, measured after randomization), BMS data was analyzed excluding those animals who scored higher than a baseline BMS of 3. Similar to above, functional recovery was not improved with administration of AM095 24 hours post-SCI. For instance, mean BMS at 54 days for AM095-treated animals was 2.90 ± 0.499 (n=10) vs. 4.545 ± 0.455 for vehicle-treated animals (n=11). Data represent means with SEM; statistical analysis was performed using GraphPad Prism and employed 2-way ANOVA.

Discussion

In conclusion, application of small molecule inhibitor of NgR1 YU-NR-008/Go did not appear to be effective in our in vitro assays or in an in vivo model of SCI. In our in vitro assays, we noted that Nogo-22 potently suppresses axonal regeneration, and this suppression was not rescued with the co-administration of Go (Fig. 4 and 6). The inhibition of axonal regeneration with Nogo-22 was expected, as noted in previous studies [58]. What has not been previously studied, however, was the effect of increasing time of exposure to Nogo-22. We show here that increasing the time of exposure to Nogo-22 increases inhibition of axonal regeneration (Fig. 4). It is unlikely that the interaction of Nogo-22 with NgR1 takes a full 7 days to reach equilibrium. Rather, in line with previous experiments that have shown an increasing capacity for Nogo-22 to suppress axonal regeneration at a greater number of days in research, it is likely that increased suppression is due to increased expression of NgR1 as cultured neurons progress through development, as noted by Huebner et al [58]. Thus, older cultures are presumably more sensitive to Nogo-22 than younger cultures [58].

It is notable that Go mediates improvement—albeit non-significant—when applied to neurons without exogenous Nogo-22 (Fig. 5). It is possible that this might be due to blockade of low levels of endogenous Nogo present in the cultures. Additionally, given the high potency of Nogo-22, it may be that, if Go were to be co-administered with lower potency Nogo-66, a reversal of inhibition could be seen. Importantly, Go-mediated improvement without the co-administration of Nogo-22 was not enhanced by increasing the number of days in culture. Theoretically, as NgR1 expression increases, so should Go-mediated disinhibition of axonal regeneration. However, increasing the number of days that Go stays in culture also renders the compound susceptible to the effects of time in the non-lipophilic culture medium. The lack of statistical

significance in our findings may suggest toxicity, precipitation of our highly lipophilic compound out of solution, or small molecule oligomerization, thus rendering it inactive for inhibition of NgR1. Of note, the precipitation of Go out of solution limited prior experiments in our laboratory (data not published). (It should also be noted that some time prior to experimentation was devoted to determining an effective mixture into which the YU-NR-008 could remain dissolved in solution, highlighting the compounds lipophilic nature.) Alternatively, other non-NgR1 related mechanisms may play an important role, indicating that inhibition of the Nogo-A/NgR1 interaction may not be sufficient in disinhibiting axonal regeneration.

Importantly, the trend in disinhibition of axonal regeneration seen with Go-treated neurons is not seen with Go co-applied with Nogo-22, indicating a lack of rescue Nogo-22-mediated inhibition of axonal regeneration. A Western blot performed to confirm the veracity of our preparation of Nogo-22 showed slight differences in band intensity as compared to original preparations of Nogo-22 (data not shown). Interestingly, the lack of disinhibition was also noted at higher doses (up to 50 μ M Go—data not shown), which also suggests that the binding of our Nogo-22 preparation may be irreversible; thus, the application of a small molecule inhibitor in an attempt to competitively antagonize Nogo-22 binding may be futile with such an experimental model. As suggested above, it would be particularly interesting to compare the inhibition resulting from Nogo-22 administration with that mediated by Nogo-66. The original DELFIA assay produced an IC₅₀ for Nogo-66 rather than Nogo-22. Importantly, Nogo-22 has been shown to induce growth cone collapse in E13 DRG neurons with a potency that is more than ten times that of Nogo-66, which suggests that Nogo-22 may bind with higher affinity to NgR1 than Nogo-66 [56]. It would therefore be interesting and important to study the competitive interaction of Go directly with Nogo-22, and to determine whether Nogo-22 or Nogo-66 accurately reflects the inhibition mediated by ligands endogenous to the neuronal environment.

Importantly, administration of the ROCK inhibitor Y27632 led to reversal to Nogo-22 mediated inhibition of axonal regeneration of cortical neurons, indicating that the ineffectiveness of YU-NR-008 in the presence of Nogo-22 likely reflects NgR1-related competition upstream from ROCK [58]. Thus, it is possible that Nogo-22 has such a slow off rate that it is essentially an irreversible inhibitor of NgR1. It is also possible that our agent YU-NR-008/Go may bind in a different location than Nogo-22. Go may thus inhibit binding of Nogo-66, but not Nogo-22 via its potentially unique binding site. Our hope is that future work might elucidate such pharmacodynamic properties of Nogo-22 and YU-NR-008.

In our behavioral studies, we did not notice any significant difference between the Go-treated and control animals when animals were treated for 2 or 4 weeks (Fig. 7). Following our two week experiment, many of the animals in either of the groups suffered complications such as hydrocephalus and urinary tract infections, thus confounding our results. Likewise, following animal sacrifice, material with the appearance of precipitated compound was noted in the peritoneum, near the site of injection. Excluding animals with ill appearance and hydrocephalus from the final data analysis yielded similar results, although by doing so the number of animals in the control group may be deemed insufficient to yield reliable results (data not shown).

Importantly, surgical technique may have also introduced a significant degree of variability from animal to animal. For animals treated for 4 weeks, one important factor that might explain the lack of functional improvement was a similar loss of animals from the control group at later time courses due to illness. Interestingly, most of the animals lost from the control group (4 out of 5) had a baseline BMS score of 0-0.5 on D3 (with the fifth animal scoring 1.0 on D3). In contrast, there were three animals lost or excluded from the Go-treated group, with baseline scores of 0, 0.5, and 3.5, respectively. As the animals were initially divided into treatment groups of equal average baseline scores, it is evident that the loss of these animals led to a selective advantage

of the control-treated vs. Go-treated animals. This likely introduced selection or attrition bias into our final analysis. Additionally, this may explain the trend to improved recovery, albeit insignificant, that is seen with the control group vs. the Go-treated animals.

The discrepancy in our results from those obtained by Wang et al through administration of the Nogo decoy receptor NgR1(310)ecto-Fc may be also be explained by the direct intrathecal administration of the latter, which—in contrast to intraperitoneal administration—may have facilitated more localized regenerative effects at the spinal cord [62]. Similarly, in contrast to the spinal cord contusion injury employed by Wang et al, our own experiments employed a partial hemisection, which—while ideal for studying neuroregeneration—can lack consistency from one animal to another [63].

With regards to the original fear extinction model which prompted further interest, the short period of treatment may have helped avoid the development of precipitation of compound in the abdomen following intraperitoneal injection (Fig. 3; unpublished). The discrepancy with our experiment also suggests that while the compound YU-NR-008 might be ideal with regards to experience-mediated effects that rely on plasticity of intact neurons, it may not be effective when more robust neuroregeneration is needed [10]. Similarly, in contrast to the relatively static expression of Nogo-A in the adult CNS, it is also important to consider the time-dependent expression of Nogo-A in the CNS following injury. The effect of time on Nogo-A expression has been extensively studied with varying results, although a more recent, perhaps more comprehensive study verified that Nogo-A mRNA expression initially falls below baseline values and reach a trough at 3 days post-SCI, indicating a permissive environment for axonal regeneration shortly after injury [28]. Soon after, however, Nogo-A expression shoots up to levels that are almost twice that of baseline, indicating that this period of permissive growth is short-lived [28]. Similar results were seen with immunohistochemistry and Western blot analysis

of tissue. Elevated levels of Nogo-A continued to be higher than baseline at two weeks post-injury [28]. Importantly, our behavioral experiments using YU-NR-008 attempted to follow a time course that relied on a three-day period of post-operative recovery and thus an accurate baseline BMS score that would allow for accurate randomization, with an initial application at 3 days post injury and a steady state reached at D4-D5. Given the above findings by Wang et al, the administration of a small molecule inhibitor of NgR1 may be optimally timed for 3-7 days post-SCI, which coincided with our experimental method [28]. It is possible, however, that the activity of other ligands might exhibit different expression patterns following injury. For example, OMgp does not show the same initial decrease as Nogo-A does following injury; rather, its expression increases steadily through 28 days following injury [64]. Importantly, NgR1 expression appears to follow a trend similar to Nogo-A following CNS injury, although the only significant difference seen vs. sham is an increase in mRNA expression 2 weeks post-injury, highlighting the relative stability of NgR1 expression—and thus capacity for RhoA/ROCK-mediated inhibition of axonal regeneration—immediately after injury [65].

It is intriguing to consider the role of the downstream effector pathway, RhoA/ROCK, in mediating inhibition of axon growth. It has been shown that in addition to suppressing axonal regeneration, the RhoA/ROCK pathway is important for maintaining polarity of growth cones [66]. Thus—similar to the importance of NgR1 in the adult human to ensure efficient and stable neuronal networks—NgR1 may be vital for guidance of new growth cones towards their appropriate targets. In light of this, while blocking NgR1 signaling may promote the propagation of growth cones shortly after administration of YU-NR-008, the activation of an additional mechanism (e.g. via external cues) might be necessary to guide newly established growth cones towards their appropriate destination [66]. Notably, NgR1 knockouts do exhibit a phenotype of more robust, functionally significant axonal recovery [67]. However, this may be accounted for

through redundant pathways that provide cues for growth cone polarity. Likewise, the effectiveness of a decoy receptor for Nogo-A also allows for the retention of NgR1 on damaged neurons, indicating that external cues relevant for polarity might act with greater nuance to allow for maintenance of effective growth cone polarity [68]. It is also possible that YU-NR-008 might not inhibit NgR1 potently enough to mirror the axonal regeneration seen with application of the decoy Nogo receptor. Histologic analysis of spinal cord tissue is forthcoming, and should show whether NgR1 led to any axonal regeneration in spite of insufficient evidence for functional recovery.

AM095

Our experiments noted that treatment with AM095 did not enhance functional recovery following SCI as compared to control. This is in contrast to previous experiments performed by Santos-Nogueira et al, where a similar dosage of AM095 was used but with treatment begun at an earlier time [44]. Santos-Nogueira et al noted that LPA levels are significantly increased from baseline starting at least 6 hours following injury [44]. Importantly, LPA and its receptors are believed to be important mediators in the inflammatory process that contributes to secondary damage in the spinal cord. The earlier this process can be inhibited, the better. Indeed, such a thought process appears to have been followed with regards to choosing an ideal time to initiate treatment: AM095 was first administered 1 hour after SCI [44]. In addition to its neuroprotective effects, however, LPA has been directly implicated in activating growth cone collapse via the RhoA/ROCK pathway. This pathway leads to the phosphorylation and thus inactivation of the myosin light chain phosphatase, thus allowing for the myosin II/actin network to contract [22]. Interestingly, Santos-Nogueira et al showed that LPA₁ was implicated in promoting demyelination in the CNS following injury [54]. A recent experiment showed that LPA also exerts its demyelinating effects through the RhoA/ROCK pathway, at least in the PNS [69].

Thus, in performing our experiments, our goal was to attempt to isolate, in part, the neuroregenerative effects of inhibiting the LPA/LPA₁ pathway. Although histological analysis needs to be performed to assess whether axon regeneration of existing neurons occurred in our experiment, the lack of a behavioral phenotype may point to a role for the otherwise ubiquitous LPA that is more important in mediating secondary injury and demyelination rather than growth cone collapse. However, a few important distinctions between our experiments warrant attention:

Whereas the experiments performed by Santos-Nogueira et al employed an impactor device to produce spinal cord contusions, our experiments employed the dorsal hemisection model [44]. Spinal cord contusion performed with validated impactor devices can limit injury variability, whereas in our experiments the experimenter's surgical technique may have introduced a significant degree of variability from animal to animal [63]. In addition, based on prior experimentation in our laboratory, it is difficult to obtain an accurate baseline BMS is difficult to achieve until 3-7 days of days following SCI. Accurate baselines are needed for adequate randomization. Animals that are scoring at a BMS of 2 the first post-operative day are likely to not have as severe an injury as animals scoring at 0 or 1. Thus, it is possible that the animals randomized to the treatment group were more severely injured (or even that the animals receiving treatment in the behavioral study performed by Santos-Nogueira et al were not as severely injured) [44]. It is also interesting to consider that neuroprotection through inhibiting inflammation may play a more important role in the contusion model, whereas functional recovery following a surgically-induced cord hemisection may rely more on axonal regeneration. Further experiments are thus required to truly disambiguate the functional significance of AM095 treatment following SCI.

Our experiments also appeared to show different results from those reported by Fink et al following AM095 treatment of animals who underwent unilateral medullary pyramidotomies (abstract submitted). In their experiments, AM095 was initially administered at the same dose (30mg/kg/12h) but at 5 hours post-pyramidotomy. This initial administration precedes the measured rise in LPA noted by Santos-Nogueira at 6 hours, which supports a neuroprotective rather than neuroregenerative role for AM095 [54]. Additionally, other experimenters have noted that the pyramidotomy is an ideal method for assessing sprouting from intact neurons [70]. Whether our animals exhibited sprouting from neurons left intact following hemisection remains to be seen on histological analysis, but it has been noted that functional recovery following medullary pyramidotomy may operate via a different pathway, i.e. μ may require a more robust neuroregenerative effect [71]. Thus, while AM095 might be ideal from a neuroprotective standpoint, its effectiveness along a spectrum of neural growth that spans from plasticity to robust regeneration of severed axons may be limited to sprouting of intact axons. Further studies that would experimentally initiate treatment of AM095 at a later time course might help to further elucidate the primary pathway by which the agent acts.

Importantly, while our results—taken with other experiments—suggest a neuroprotective rather than neuroregenerative role for AM095, it is important to emphasize that it can be difficult to delineate between the two phenomena. Neuroprotection effectively inhibits the formation of scar tissue, which—acting via CSPGs—has been shown to inhibit neuroregeneration [10, 72]. Thus, while there is evidence to suggest that contralateral sprouting in animals who received pyramidotomies may occur following administration of AM095, without altering the time course of treatment, it may be difficult to attribute such sprouting to neuroregeneration. Given the potential effect of neuroprotection, it is interesting to consider the potentially additive effect of administering AM095 (or other LPA₁ antagonist) immediately

following spinal cord injury and following this with administration of an NgR1 antagonist at a time that coincides with Nogo-A expression post-SCI, e.g. 2-3 days following injury [28]. In this way, one could inhibit the inflammatory cascade that is likely detrimental to neurons and associated myelin while disinhibiting the outgrowth of axons to allow for functional recovery. Likewise, if inhibition of the LPA₁ pathway was confirmed to facilitate axonal regeneration (as suggested by previous research), the additive effects of inhibiting LPA₁ and NgR1 signaling may provide for a more robust cellular and functional recovery than either compound alone. Further research may help to elucidate the interaction of these two proposed mechanisms of CNS recovery following injury, and bring us closer to much-needed treatments for CNS injury.

References

1. *Spinal cord injury facts and figures at a glance*. J Spinal Cord Med, 2014. **37**(4): p. 479-80.
2. Chang, H.K., A. Veeravagu, and M.Y. Wang, *Neuroregeneration: North America's First Human Stem Cell Trial for Stroke*. Neurosurgery, 2016. **79**(6): p. N21-N22.
3. Liu, B.P., et al., *Extracellular regulators of axonal growth in the adult central nervous system*. Philosophical Transactions of the Royal Society B-Biological Sciences, 2006. **361**(1473): p. 1593-1610.
4. Lutz, A.B. and B.A. Barres, *Contrasting the Glial Response to Axon Injury in the Central and Peripheral Nervous Systems*. Developmental Cell, 2014. **28**(1): p. 7-17.
5. Aguayo, A.J., S. David, and G.M. Bray, *Influences of the Glial Environment on the Elongation of Axons after Injury - Transplantation Studies in Adult Rodents*. Journal of Experimental Biology, 1981. **95**(Dec): p. 231-&.
6. Windle, W.F., *Regeneration of Axons in the Vertebrate Central Nervous System*. Physiological Reviews, 1956. **36**(4): p. 427-440.
7. Morgenstern, D.A., R.A. Asher, and J.W. Fawcett, *Chondroitin sulphate proteoglycans in the CNS injury response*. Spinal Cord Trauma: Regeneration, Neural Repair and Functional Recovery, 2002. **137**: p. 313-332.
8. Bernstein, J.J. and M.E. Bernstein, *Axonal Regeneration and Formation of Synapses Proximal to Site of Lesion Following Hemisection of Rat Spinal Cord*. Exp Neurol, 1971. **30**(2): p. 336-+.
9. Savio, T. and M.E. Schwab, *Rat Cns White Matter, but Not Gray-Matter, Is Nonpermissive for Neuronal Cell-Adhesion and Fiber Outgrowth*. Journal of Neuroscience, 1989. **9**(4): p. 1126-1133.
10. Huebner, E.A. and S.M. Strittmatter, *Axon Regeneration in the Peripheral and Central Nervous Systems*. Cell Biology of the Axon, 2009. **48**: p. 339-351.
11. Atwal, J.K., et al., *PirB is a Functional Receptor for Myelin Inhibitors of Axonal Regeneration*. Science, 2008. **322**(5903): p. 967-970.
12. Geoffroy, C.G. and B.H. Zheng, *Myelin-associated inhibitors in axonal growth after CNS injury*. Current Opinion in Neurobiology, 2014. **27**: p. 31-38.
13. Wang, X., et al., *Localization of Nogo-A and Nogo-66 receptor proteins at sites of axon-myelin and synaptic contact*. J Neurosci, 2002. **22**(13): p. 5505-15.
14. Kim, J.E., et al., *Nogo-66 receptor prevents raphespinal and rubrospinal axon regeneration and limits functional recovery from spinal cord injury*. Neuron, 2004. **44**(3): p. 439-451.
15. Wang, K.C., et al., *p75 interacts with the Nogo receptor as a co-receptor for Nogo, MAG and OMgp*. Nature, 2002. **420**(6911): p. 74-78.
16. Dickendesher, T.L., et al., *NgR1 and NgR3 are receptors for chondroitin sulfate proteoglycans*. Nat Neurosci, 2012. **15**(5): p. 703-712.
17. Sivasankaran, R., et al., *PKC mediates inhibitory effects of myelin and chondroitin sulfate proteoglycans on axonal regeneration*. Nat Neurosci, 2004. **7**(3): p. 261-268.
18. Fournier, A.E., B.T. Takizawa, and S.M. Strittmatter, *Rho kinase inhibition enhances axonal regeneration in the injured CNS*. Journal of Neuroscience, 2003. **23**(4): p. 1416-1423.
19. Nakagawa, O., et al., *ROCK-I and ROCK-II, two isoforms of Rho-associated coiled-coil forming protein serine/threonine kinase in mice*. Febs Letters, 1996. **392**(2): p. 189-193.

20. Gallo, G. and P.C. Letourneau, *Regulation of growth cone actin filaments by guidance cues*. J Neurobiol, 2004. **58**(1): p. 92-102.
21. Gallo, G., *RhoA-kinase coordinates F-actin organization and myosin II activity during semaphorin-3A-induced axon retraction*. J Cell Sci, 2006. **119**(Pt 16): p. 3413-23.
22. Schmidt, J.T., et al., *Myosin light chain phosphorylation and growth cone motility*. J Neurobiol, 2002. **52**(3): p. 175-88.
23. Akbik, F.V., et al., *Anatomical plasticity of adult brain is titrated by Nogo Receptor 1*. Neuron, 2013. **77**(5): p. 859-66.
24. Bartsch, U., et al., *Lack of evidence that myelin-associated glycoprotein is a major inhibitor of axonal regeneration in the CNS*. Neuron, 1995. **15**(6): p. 1375-1381.
25. Dimou, L., et al., *Nogo-A-deficient mice reveal strain-dependent differences in axonal regeneration*. Journal of Neuroscience, 2006. **26**(21): p. 5591-5603.
26. Lee, J.K., et al., *Assessing Spinal Axon Regeneration and Sprouting in Nogo-, MAG-, and OMgp-Deficient Mice*. Neuron, 2010. **66**(5): p. 663-670.
27. Wang, T., et al., *The role of Nogo-A in neuroregeneration: A review*. Brain Research Bulletin, 2012. **87**(6): p. 499-503.
28. Wang, J.W., et al., *Nogo-A expression dynamically varies after spinal cord injury*. Neural Regen Res, 2015. **10**(2): p. 225-9.
29. Hu, F.H. and S.M. Strittmatter, *The N-terminal domain of Nogo-A inhibits cell adhesion and axonal outgrowth by an integrin-specific mechanism*. Journal of Neuroscience, 2008. **28**(5): p. 1262-1269.
30. Huber, A.B., et al., *Patterns of Nogo mRNA and protein expression in the developing and adult rat and after CNS lesions*. J Neurosci, 2002. **22**(9): p. 3553-67.
31. Bouton, C.E., et al., *Restoring cortical control of functional movement in a human with quadriplegia*. Nature, 2016. **533**(7602): p. 247-50.
32. Hunt, D., R.S. Coffin, and P.N. Anderson, *The Nogo receptor, its ligands and axonal regeneration in the spinal cord; a review*. J Neurocytol, 2002. **31**(2): p. 93-120.
33. Li, S.X., et al., *Blockade of Nogo-66, myelin-associated glycoprotein, and oligodendrocyte myelin glycoprotein by soluble Nogo-66 receptor promotes axonal sprouting and recovery after spinal injury*. Journal of Neuroscience, 2004. **24**(46): p. 10511-10520.
34. Wang, X.X., et al., *Recovery from chronic spinal cord contusion after nogo receptor intervention*. Annals of Neurology, 2011. **70**(5): p. 805-821.
35. Bregman, B.S., et al., *Recovery from Spinal-Cord Injury Mediated by Antibodies to Neurite Growth-Inhibitors*. Nature, 1995. **378**(6556): p. 498-501.
36. Griesbach, G.S. and D.A. Hovda, *Cellular and molecular neuronal plasticity*. Handb Clin Neurol, 2015. **128**: p. 681-90.
37. Bhagat, S.M., et al., *Erasure of fear memories is prevented by Nogo Receptor 1 in adulthood*. Mol Psychiatry, 2016. **21**(9): p. 1281-9.
38. Neves, G., S.F. Cooke, and T.V. Bliss, *Synaptic plasticity, memory and the hippocampus: a neural network approach to causality*. Nature Reviews Neuroscience, 2008. **9**(1): p. 65-75.
39. Mehta, M.R., *From synaptic plasticity to spatial maps and sequence learning*. Hippocampus, 2015. **25**(6): p. 756-62.
40. Zemmar, A., et al., *Neutralization of Nogo-A enhances synaptic plasticity in the rodent motor cortex and improves motor learning in vivo*. J Neurosci, 2014. **34**(26): p. 8685-98.
41. Maren, S., *Neurobiology of Pavlovian fear conditioning*. Annu Rev Neurosci, 2001. **24**: p. 897-931.

42. Myers, K.M. and M. Davis, *Mechanisms of fear extinction*. Mol Psychiatry, 2007. **12**(2): p. 120-50.
43. Gogolla, N., et al., *Perineuronal nets protect fear memories from erasure*. Science, 2009. **325**(5945): p. 1258-61.
44. Santos-Nogueira, E., et al., *Activation of Lysophosphatidic Acid Receptor Type 1 Contributes to Pathophysiology of Spinal Cord Injury*. Journal of Neuroscience, 2015. **35**(28): p. 10224-10235.
45. Pruss, H., et al., *Non-Resolving Aspects of Acute Inflammation after Spinal Cord Injury (SCI): Indices and Resolution Plateau*. Brain Pathology, 2011. **21**(6): p. 652-660.
46. Zhang, B. and J.C. Gensel, *Is neuroinflammation in the injured spinal cord different than in the brain? Examining intrinsic differences between the brain and spinal cord*. Exp Neurol, 2014. **258**: p. 112-120.
47. Bloom, O., *Non-mammalian model systems for studying neuro-immune interactions after spinal cord injury*. Exp Neurol, 2014. **258**: p. 130-40.
48. Anthony, D.C. and Y. Couch, *The systemic response to CNS injury*. Exp Neurol, 2014. **258**: p. 105-11.
49. Schwab, J.M., et al., *The paradox of chronic neuroinflammation, systemic immune suppression, autoimmunity after traumatic chronic spinal cord injury (vol 258, pg 121, 2014)*. Exp Neurol, 2014. **261**: p. 540-540.
50. Plemel, J.R., V.W. Yong, and D.P. Stirling, *Immune modulatory therapies for spinal cord injury - Past, present and future*. Exp Neurol, 2014. **258**: p. 91-104.
51. Stirling, D.P., et al., *Depletion of Ly6G/Gr-1 Leukocytes after Spinal Cord Injury in Mice Alters Wound Healing and Worsens Neurological Outcome*. Journal of Neuroscience, 2009. **29**(3): p. 753-764.
52. Shechter, R., et al., *Infiltrating Blood-Derived Macrophages Are Vital Cells Playing an Anti-inflammatory Role in Recovery from Spinal Cord Injury in Mice*. Plos Medicine, 2009. **6**(7).
53. Yung, Y.C., N.C. Stoddard, and J. Chun, *LPA receptor signaling: pharmacology, physiology, and pathophysiology*. Journal of Lipid Research, 2014. **55**(7): p. 1192-214.
54. Santos-Nogueira, E., et al., *Activation of Lysophosphatidic Acid Receptor Type 1 Contributes to Pathophysiology of Spinal Cord Injury*. J Neurosci, 2015. **35**(28): p. 10224-35.
55. Choi, J.W. and J. Chun, *Lysophospholipids and their receptors in the central nervous system*. Biochim Biophys Acta, 2013. **1831**(1): p. 20-32.
56. Swaney, J.S., et al., *Pharmacokinetic and Pharmacodynamic Characterization of an Oral Lysophosphatidic Acid Type 1 Receptor-Selective Antagonist*. Journal of Pharmacology and Experimental Therapeutics, 2011. **336**(3): p. 693-700.
57. Lee, C.W., et al., *LPA(4)/GPR23 is a lysophosphatidic acid (LPA) receptor utilizing G(s)-, G(q)/G(i)-mediated calcium signaling and G(12/13)-mediated Rho activation*. J Biol Chem, 2007. **282**(7): p. 4310-7.
58. Huebner, E.A., et al., *A multi-domain fragment of Nogo-A protein is a potent inhibitor of cortical axon regeneration via Nogo receptor 1*. J Biol Chem, 2011. **286**(20): p. 18026-36.
59. Basso, D.M., et al., *Basso Mouse Scale for locomotion detects differences in recovery after spinal cord injury in five common mouse strains*. J Neurotrauma, 2006. **23**(5): p. 635-59.
60. Hill, R.L., et al., *Anatomical and functional outcomes following a precise, graded, dorsal laceration spinal cord injury in C57BL/6 mice*. J Neurotrauma, 2009. **26**(1): p. 1-15.

61. Lang, C., et al., *Single collateral reconstructions reveal distinct phases of corticospinal remodeling after spinal cord injury*. PLoS One, 2012. **7**(1): p. e30461.
62. Wang, X., et al., *Recovery from chronic spinal cord contusion after Nogo receptor intervention*. Annals of Neurology, 2011. **70**(5): p. 805-21.
63. Cheriyan, T., et al., *Spinal cord injury models: a review*. Spinal Cord, 2014. **52**(8): p. 588-95.
64. Dou, F.F., et al., *Temporospatial Expression and Cellular Localization of Oligodendrocyte Myelin Glycoprotein (OMgp) after Traumatic Spinal Cord Injury in Adult Rats*. Journal of Neurotrauma, 2009. **26**(12): p. 2299-2311.
65. Ukai, J., et al., *Nogo receptor 1 is expressed in both primary cultured glial cells and neurons*. Nagoya J Med Sci, 2016. **78**(3): p. 303-11.
66. Loudon, R.P., et al., *RhoA-kinase and myosin II are required for the maintenance of growth cone polarity and guidance by nerve growth factor*. J Neurobiol, 2006. **66**(8): p. 847-67.
67. Huebner, E.A. and S.M. Strittmatter, *Axon regeneration in the peripheral and central nervous systems*. Results Probl Cell Differ, 2009. **48**: p. 339-51.
68. Li, S., et al., *Blockade of Nogo-66, myelin-associated glycoprotein, and oligodendrocyte myelin glycoprotein by soluble Nogo-66 receptor promotes axonal sprouting and recovery after spinal injury*. J Neurosci, 2004. **24**(46): p. 10511-20.
69. Tsukahara, R. and H. Ueda, *Myelin-related gene silencing mediated by LPA1 - Rho/ROCK signaling is correlated to acetylation of NFKappaB in S16 Schwann cells*. J Pharmacol Sci, 2016. **132**(2): p. 162-165.
70. Kathe, C., et al., *Unilateral pyramidotomy of the corticospinal tract in rats for assessment of neuroplasticity-inducing therapies*. J Vis Exp, 2014(94).
71. Lee, D.H. and J.K. Lee, *Animal models of axon regeneration after spinal cord injury*. Neurosci Bull, 2013. **29**(4): p. 436-44.
72. Onose, G., et al., *A review of published reports on neuroprotection in spinal cord injury*. Spinal Cord, 2009. **47**(10): p. 716-726.
73. Lee, J.Y. and S. Petratos, *Multiple Sclerosis: Does Nogo Play a Role?* Neuroscientist, 2013. **19**(4): p. 394-408.
74. Lauren, J., et al., *Characterization of myelin ligand complexes with neuronal Nogo-66 receptor family members*. J Biol Chem, 2007. **282**(8): p. 5715-25. This research [i.e. crystal structure figure] was originally published in Journal of Biological Chemistry. Lauren, J. et al. Title. *Characterization of myelin ligand complexes with neuronal Nogo-66 receptor family members*. 2007; **282**(8): p. 5715-25. © the American Society for Biochemistry and Molecular Biology.

Figure References and Legends

Figure 1.

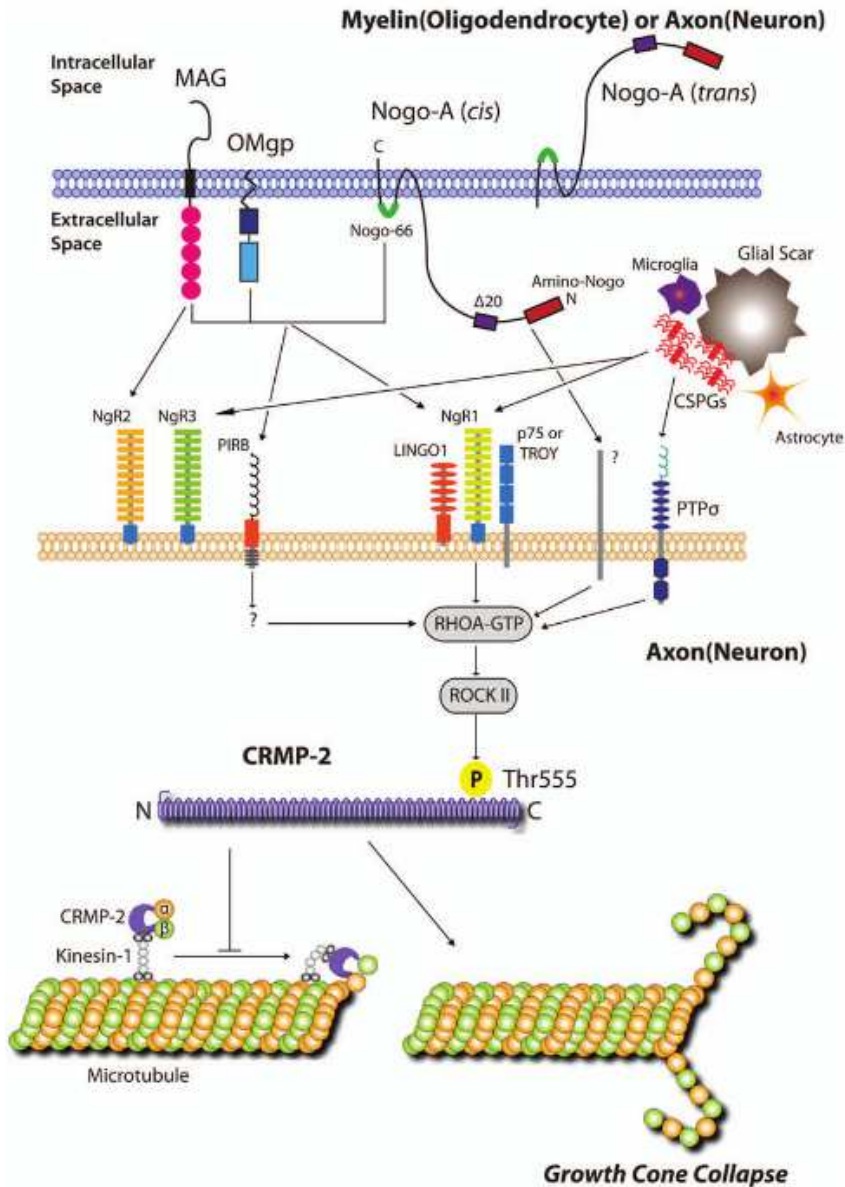


Figure 1. *NgR1* signaling pathway. (Figure from JY Lee et al 2013). Nogo-A, Oligodendrocyte Myelin Glycoprotein (OMgp), myelin-associated glycoprotein (MAG) have been shown to interact with the neuronal Nogo-66 Receptor 1 (NgR1) as well as paired-immunoglobulin like receptor B (PirB), both of which have been implicated in inhibition of axonal outgrowth. When

NgR1 is bound to ligand (which may include CSPGs), a complex is formed with the co-receptors/signal transducers LINGO-1 and p75^{NTR} or TAJ/TROY, which—possibly via protein kinase C—ultimately activates the RhoA/ROCK pathway. Activation of the RhoA/ROCK pathway leads to actin regulation and concomitant growth cone collapse and inhibition of neurite outgrowth, thus prohibiting neuroregeneration of damaged neuronal processes or sprouting of fibers from intact axons [73].

Figure 2.

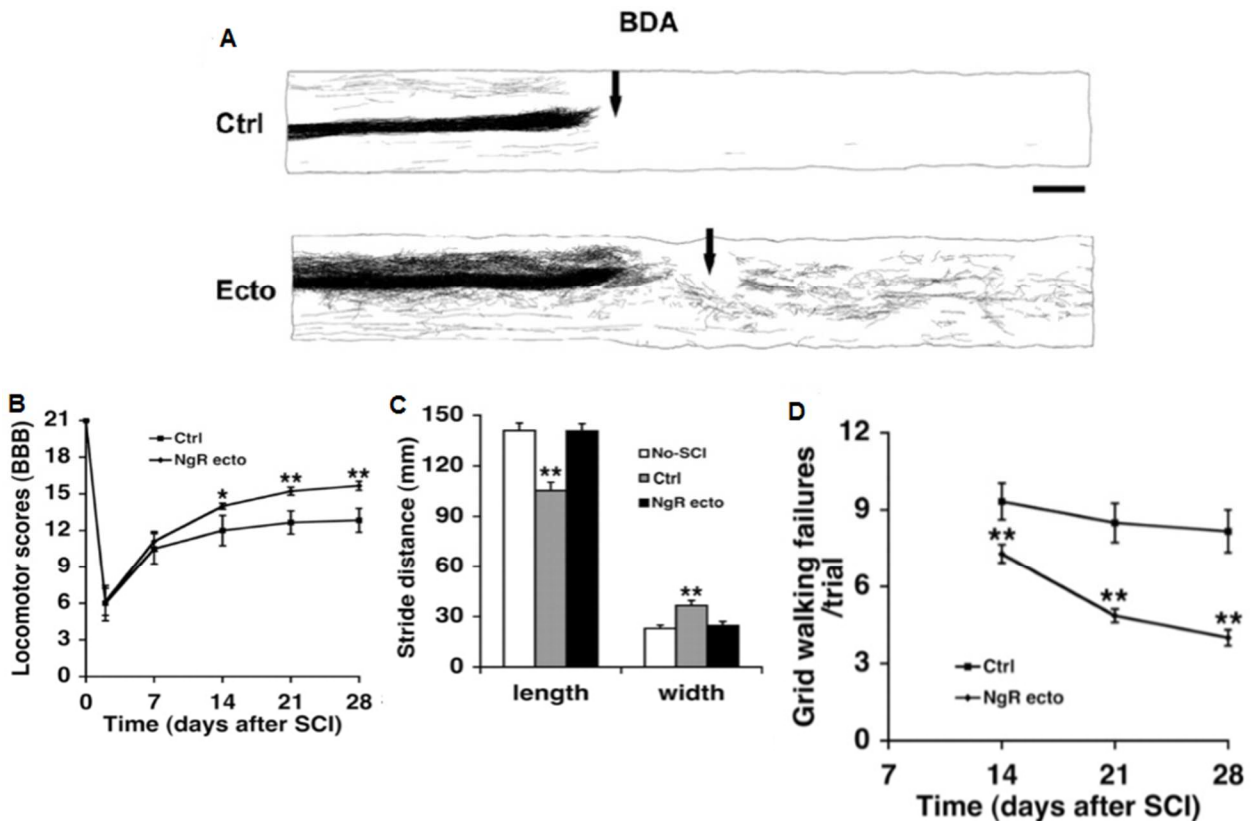


Figure 2. The Nogo decoy receptor *NgR(310)ecto-Fc* enhances the growth of CST fibers in a functionally significant manner. (Images courtesy of Lin et al 2004) **A** An example of two camera lucida drawings from rat spinal cords following biotinylated dextran amine (BDA) injections into the sensorimotor cortex of the brain show that *NgR(310)ecto-Fc* treated rats exhibit greater sprouting caudal to the site of the lesion (indicated by the black arrow). **B** Intrathecal administration of *NgR(310)ecto-Fc* promotes functional recovery following dorsal hemisection as measured by the Basso, Beattie and Bresnahan Locomotor Score for rats. 7-9 rats per group received dorsal overhemisection with subsequent intrathecal administration of vehicle or *NgR(310)ecto-Fc*. BBB at 21d was 15.5 ± 0.2 ($p < 0.01$) for *NgR(310)ecto-Fc* treated animals and 12.5 ± 0.9 for control. This experiment was repeated two more times (once at a different

institution) with similar significant results. **C** Control animals are noted to have significantly shorter strides with wider stance at 4 weeks following injury as compared to NgR(310)ecto-Fc treated animals or animals without SCI. **D** Rats treated with NgR(310)ecto-Fc have notably less hindlimb errors 2, 3, and 4 weeks following SCI [33].

Figure 3.

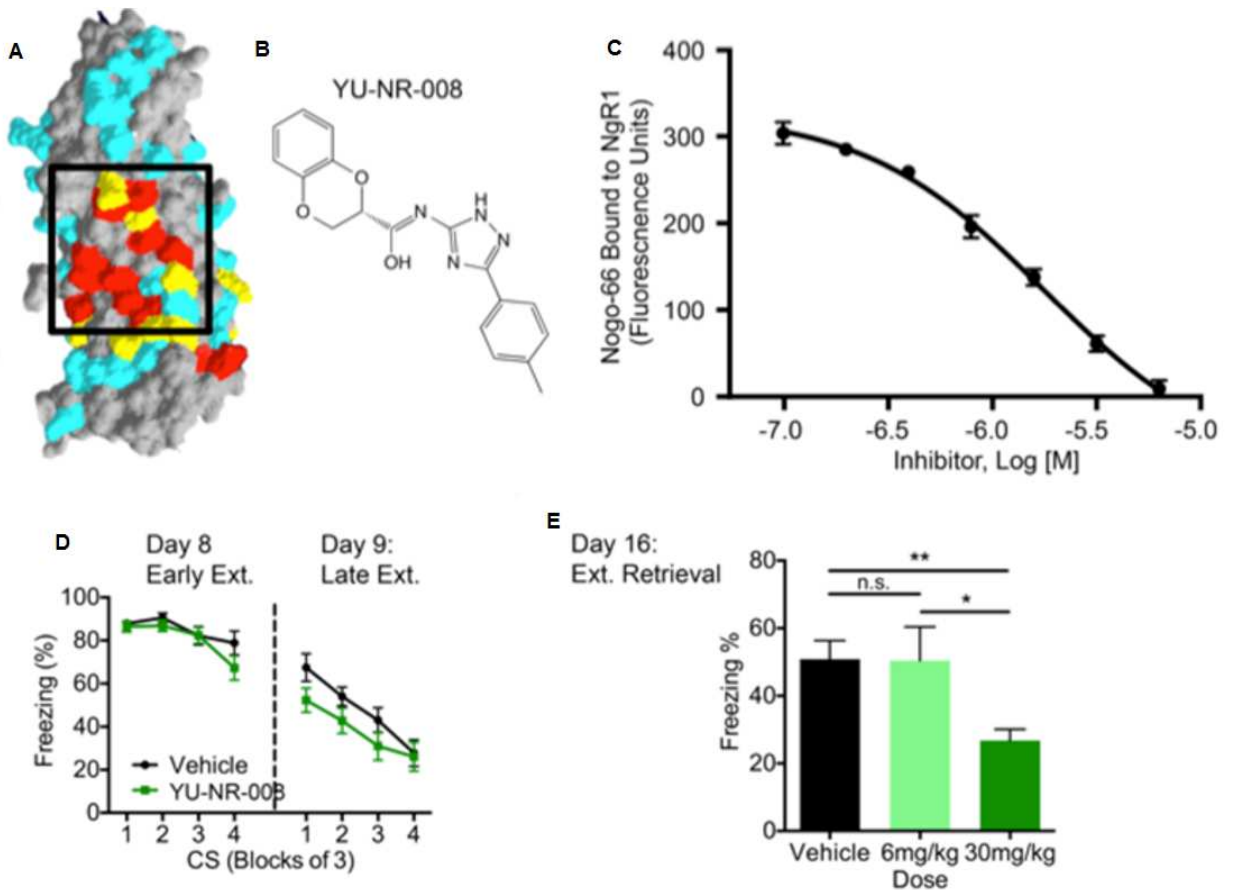


Figure 3. YU-NR-008, a small molecule Inhibitor of NgR1, shows promise in a rodent model of neuroplasticity. (Figure and data courtesy of Kalp, Bhagat et al, unpublished). **A** Crystal structure as elucidated by J. Lauren et al showing residues critical for binding of all three primary myelin-associated inhibitors (MAI; i.e. MAG, OMgp, and Nogo-A) shown in red, residues required for some, but not all MAI in yellow, and non-essential residues shown in turquoise. The black box was used for *in silico* compound screening [74]. **B** The biochemical structure of YU-NR-008, also known as "Go". **C** A DELFIA assay showing the dose response curve for YU-NR-008-mediated antagonism of Nogo-66 binding to immobilized NgR(310)ecto-Fc. **D** One day following fear conditioning, mice received 30 mg/kg/12h YU-NR-008 intraperitoneally (n=10) or vehicle (n=10) and showed similar rates of fear extinction. **E** However, mice treated with the drug showed a

significant decrease in fear recovery vs. control as measured by percentage of mice showing the fear response. Data represent the means with SEM for vehicle treated (n=19), 6 mg/kg/12h YU-NR-008 (n=8) or 30 mg/kg/12h YU-NR-008 (n=20) as measured by ANOVA with Bonferroni corrected *post hoc* analysis. *P<0.05, **P<0.01.

Figure 4.

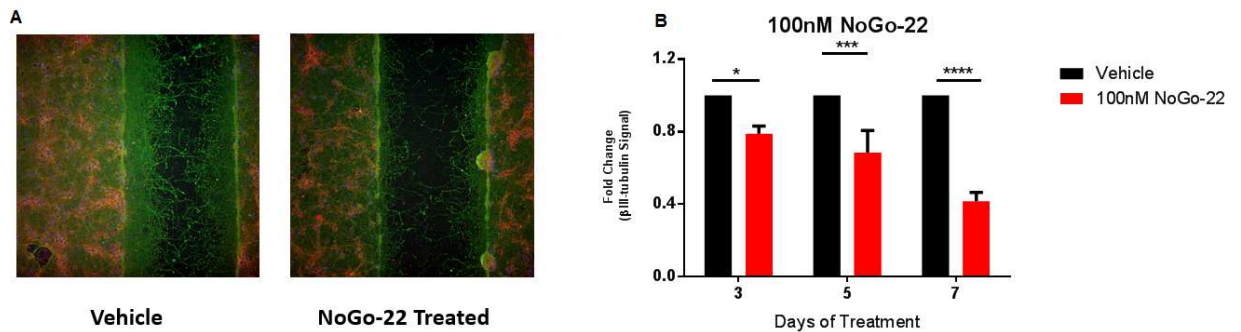


Figure 4. *Nogo-22 is a potent inhibitor of axonal regeneration.* **A** is a representative image showing Nogo-22 mediated inhibition on axonal regeneration into the scrape area vs. control. **B** As expected, Nogo-22 potently inhibits axonal regeneration when applied for three (0.788±0.043 for Nogo-22-treated (n=16) and 1.00±0.00 (n=20) for vehicle-treated (data are normalized), five (0.683±0.123 for Nogo-22 (n=16) and 1.00±0.00 for vehicle; n=16) and seven days (0.416±0.049 for Nogo-22 (n=8) and 1.00±0.00 for vehicle treated; n=8). Data represent relative intensity of signal normalized to vehicle from a fluorescent antibody to β-III tubulin (found in axons) and are displayed as means with standard errors of the mean and were analyzed by 2-Way ANOVA using GraphPad Prism statistical software. *p<0.05; ***p<0.001; ****p<0.0001

Figure 5.

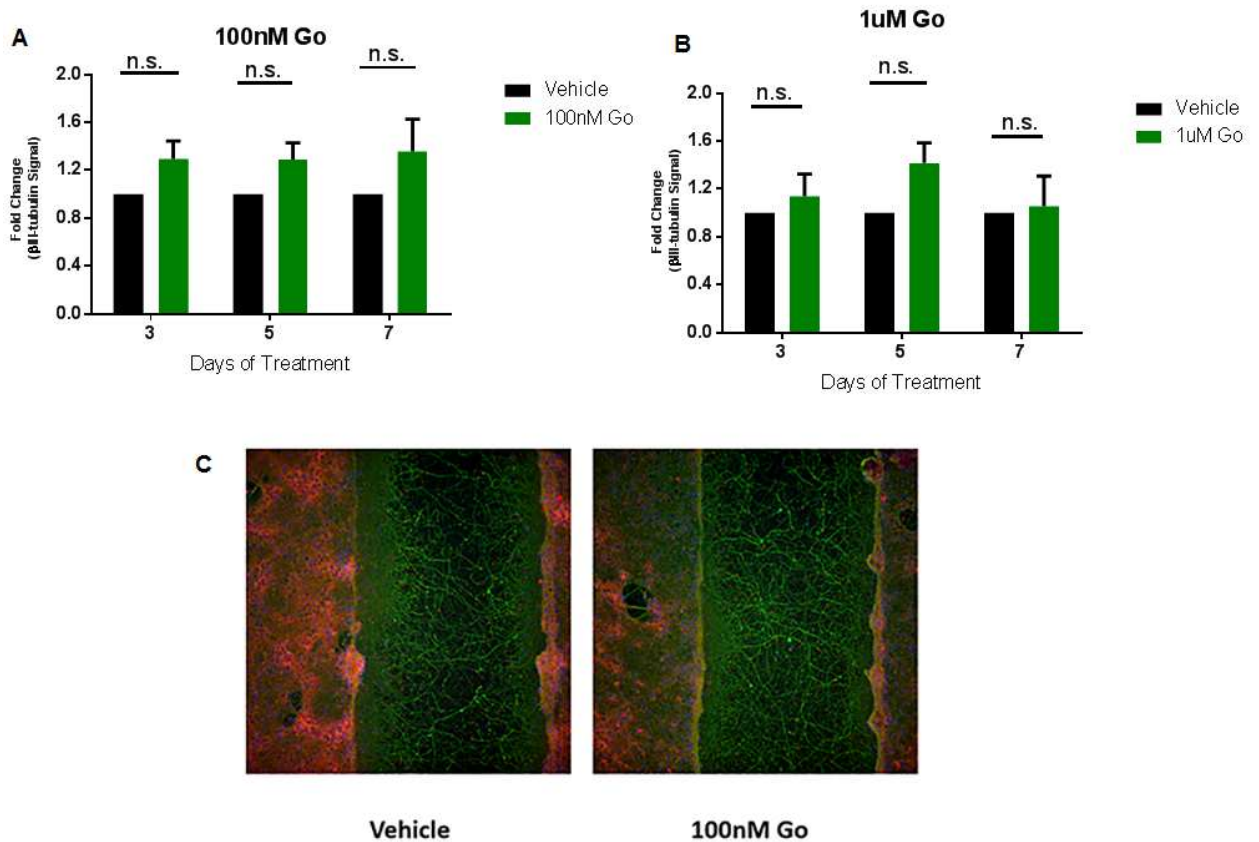


Figure 5. *Go* is non-toxic to neurons. **A** 100nM of YU-NR-008 treatment of cortical neurons at 7DIV for 3, 5 and 7 days shows a trend towards improvement in axonal regeneration as compared to control, although this trend is not significant. At 3 days of treatment, Go-treated neurons showed a relative β -III tubulin signal of 1.296 ± 0.150 ($n=16$) vs. vehicle treated (1.000 ± 0.000 ; $n=12$). At 5 days, Go-treated neurons were 1.290 ± 0.140 ($n=12$) vs. vehicle treated (1.000 ± 0.000 ; $n=8$). At 7 days, Go-treated neurons were 1.357 ± 0.271 ($n=4$) vs. 1.000 ± 0.000 for vehicle-treated ($n=4$). **B** Similarly, increasing the concentration of Go to $1\mu\text{M}$ and applying to cultures at 7DIV for varying days of treatment did not yield significant improvement in axonal regeneration. At 3 days of treatment, treatment with $1\mu\text{M}$ Go yielded a mean signal intensity of 1.140 ± 0.184 ($n=8$) vs. vehicle (1.000 ± 0.000 ; $n=8$). At 5 days, Go-treated showed a mean signal

intensity of 1.417 ± 0.167 (n=12) vs. control (1.000 ± 0.000 ; n=8). At 7 days, Go-treated were 1.054 ± 0.253 (n=4) vs. vehicle (1.000 ± 0.000 ; n=4). Data represent relative intensity of signal from a fluorescent antibody to β -III tubulin (found in axons), normalized to vehicle, and are displayed as means with standard errors of the mean and were analyzed by 2-Way ANOVA using GraphPad Prism statistical software. **C** is a representative image showing the increase in axonal regeneration with Go application.

Figure 6.

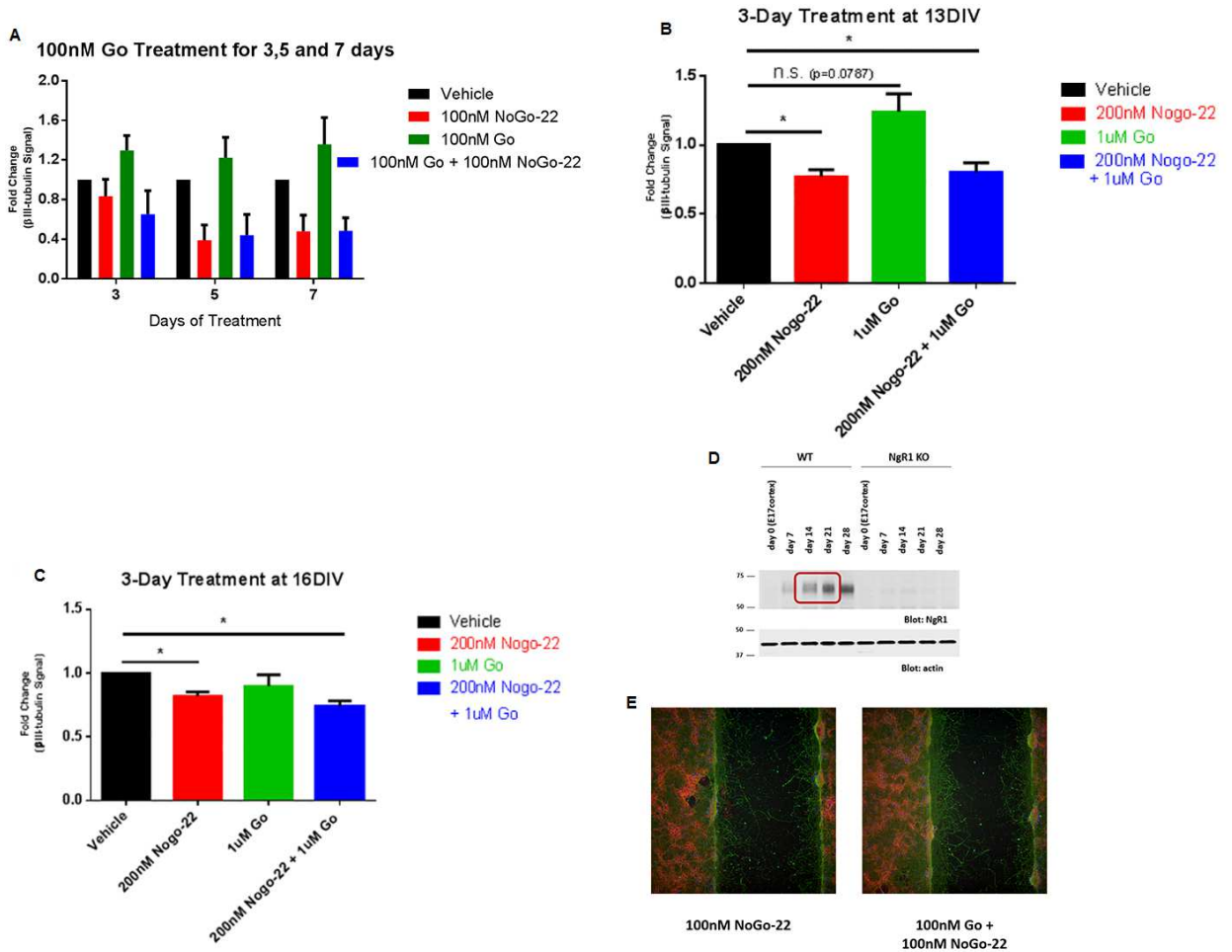


Figure 6. *Go* does not rescue Nogo-22-mediated inhibition of axonal regeneration. **A** As shown, treatment with 100nM *Go* at 3, 5, and 7 days does not rescue inhibition of axonal regeneration vs. control, although a trend exists (green bar). However, co-treatment with *Go* and Nogo-22 does not appear to rescue Nogo-22-mediated inhibition of axonal regeneration (blue bar). For example, at 7 days of treatment, neurons co-treated with *Go* and Nogo-22 (0.484 ± 0.066 ; $n=4$) and Nogo-22 alone (0.480 ± 0.082) experienced a similar inhibition of axonal regeneration. **B** 3-day treatment with *Go* at 13 DIV. Treatment with Nogo-22 yields significant inhibition (Nogo-22 0.771 ± 0.051 (SEM) vs. control 1.00 ± 0.00 , $p=0.00434$). Application of the NgR1 inhibitor *Go*

on its own showed a trend toward improved axonal regeneration, albeit insignificant (Go 1.243 ± 0.128 vs. control 1.00 ± 0.00 , $p = 0.0787$). Co-treatment with Go and Nogo-22 did not rescue Nogo-22-mediated inhibition of axonal regeneration (Nogo-22 0.771 ± 0.051 vs. Nogo-22 with Go 0.801 ± 0.073). **C** Increasing the number of days in vitro to 16 followed by treatment with Go does shows similar results: 0.820 ± 0.033 ($n=3$) for Nogo-22 alone (red column) vs. 0.899 ± 0.089 ($n=3$) for Go-treated (green column) vs. 0.737 ± 0.046 for Go with Nogo-22 ($n=3$) vs. 1.000 ± 0.000 ($n=3$) for vehicle-treated. Data represent relative intensity of signal from a fluorescent antibody to β -III tubulin (found in axons), normalized to vehicle-treated, and are displayed as means with standard errors of the mean and were analyzed by 2-Way ANOVA using GraphPad Prism statistical software. **D** A Western blot showing the rationale for attempting experiment optimization by increasing the number of DIV. As shown, NgR1 expression increases with time, although neuroregeneration becomes substantially inhibited the older neurons are (Figure unpublished, courtesy of Yuichi Sekine, PhD. Similar findings are noted in Huebner et al [58]. **E** A representative image showing the difference in regeneration with Nogo-22 alone vs. simultaneous treatment with 100nM Go. * $p < 0.05$

Figure 7.

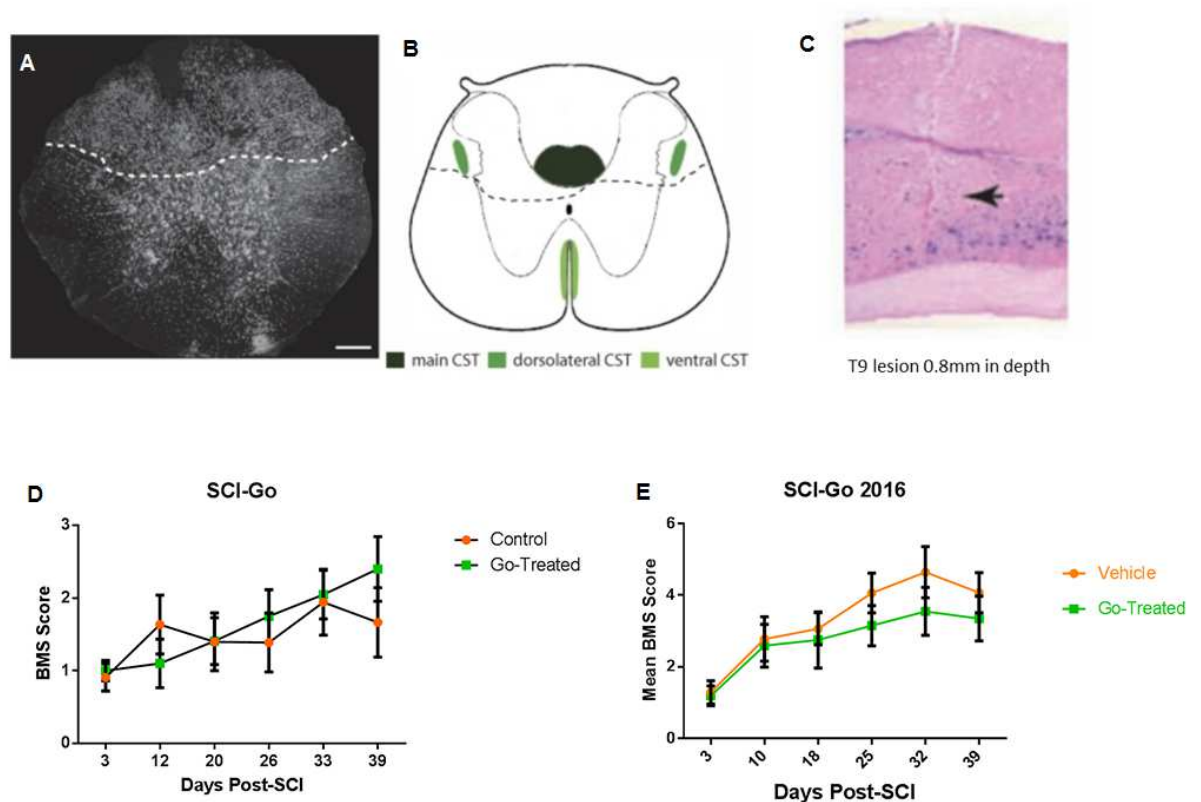


Figure 7. Treatment with Go does not promote functional recovery in spinal cord injury. **A** A representative image from Lang et al. shows a cross section of a mouse spinal cord from level T8, using Neurotrace (ThermoFisher Scientific) as a counterstain. The dotted line shows the area of intended transection using microscissors [61]. **B** As shown in this image from Lang et al, the goal of the dorsal hemisection is to transect the main CST to ensure that recovery of function is associated with regeneration rather than retention of main CST fibers [61]. The baseline Basso Mouse Scale (BMS) score affords a functional measurement of the effectiveness of the dorsal hemisection. **C** Cresyl violet- and eosin-stained section showing a representative lesion using a precise incision device [60]. For our experiments, microscissors were employed using a similar

depth of injury (0.8-1.1mm). **D** Mean BMS scores for mice treated with control or NgR1 inhibitor at D3 after dorsal hemisection. As shown, animals are divided into groups with a similar mean baseline score. 2-week treatment with Go at 30mg/kg/12hr did not appear to promote functional recovery following dorsal hemisection as measured by the BMS. For instance, at D39 mean BMS for Go-treated animals was 2.40 ± 0.46 (n=10) vs. 1.667 ± 0.479 for control (n=9). Continuing the experiment for one more week yielded similar results (data not shown). **E** 4-week treatment with Go at 30mg/kg/12hr did not appear to promote functional CNS recovery following dorsal hemisection. For example, the differences between D32 BMS scores (4.643 ± 0.713 (SEM) for control vs. 3.550 ± 0.669 for Go-treated animals) or D39 (4.071 ± 0.561 (control) vs. 3.35 ± 0.624) were not significant. Data represent means with SEM; statistical analysis was performed using GraphPad Prism and employed 2-way ANOVA.

Figure 8.

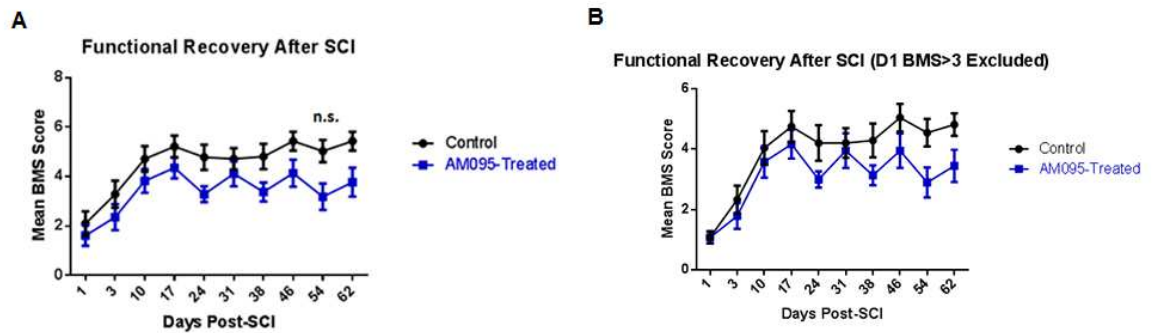


Figure 8. Treatment with AM095 starting 24 hours after spinal cord injury does not appear to promote functional recovery. **A** As shown, treatment with the LPA₁ antagonist AM095 starting 24 hours after injury did not appear to yield improvement in functional recovery as measured by the Basso Mouse Scale (BMS). For example, mean BMS at 54 days for AM095-treated animals was 3.182 ± 0.532 (n=11) vs. 5.033 ± 0.448 for vehicle-treated animals (n=15). **B** Given the potential for skewed data with a disproportionate number of abnormally high baseline performers (as in D3 baseline, measured after randomization), BMS data was analyzed excluding those animals who scored higher than a baseline BMS of 3. Similar to above, functional recovery was not improved with administration of AM095 24 hours post-SCI. For instance, mean BMS at 54 days for AM095-treated animals was 2.90 ± 0.499 (n=10) vs. 4.545 ± 0.455 for vehicle-treated animals (n=11). Data represent means with SEM; statistical analysis was performed using GraPad Prism and employed 2-way ANOVA.